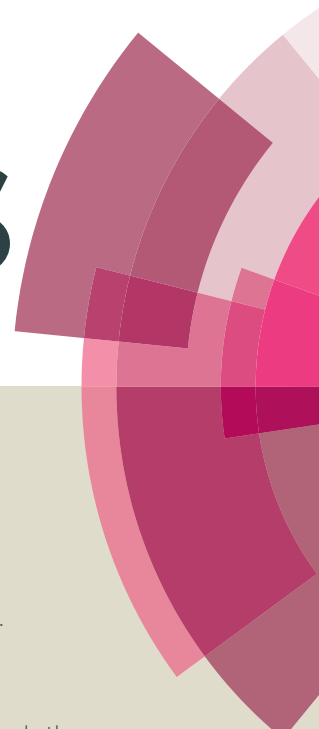


RSC Advances



This article can be cited before page numbers have been issued, to do this please use: V. L. Sharma, D. Mandalapu, D. K. Singh, S. Gupta, V. M. Balaramnavar, M. Shafiq and D. Banerjee, *RSC Adv.*, 2016, DOI: 10.1039/C5RA25853G.



This is an *Accepted Manuscript*, which has been through the Royal Society of Chemistry peer review process and has been accepted for publication.

Accepted Manuscripts are published online shortly after acceptance, before technical editing, formatting and proof reading. Using this free service, authors can make their results available to the community, in citable form, before we publish the edited article. This *Accepted Manuscript* will be replaced by the edited, formatted and paginated article as soon as this is available.

You can find more information about *Accepted Manuscripts* in the [Information for Authors](#).

Please note that technical editing may introduce minor changes to the text and/or graphics, which may alter content. The journal's standard [Terms & Conditions](#) and the [Ethical guidelines](#) still apply. In no event shall the Royal Society of Chemistry be held responsible for any errors or omissions in this *Accepted Manuscript* or any consequences arising from the use of any information it contains.



Journal Name

Paper

Discovery of monocarbonyl curcumin hybrids as a novel class of human DNA ligase I inhibitors: *In silico* design, synthesis and biology[#]

Received 00th January 20xx,
Accepted 00th January 20xx

DOI: 10.1039/x0xx00000x

www.rsc.org/

Dhanaraju Mandalapu,^{§,a} Deependra Kumar Singh,^{§,b} Sonal Gupta,^{a,c} Vishal M. Baramnavar,^{b,1} Mohammad Shafiq,^b Dibyendu Banerjee^{*,b,c} and Vishnu Lal Sharma^{*,b,c}

A pharmacophore model was generated and validated by using known human DNA ligase inhibitors for the identification of a novel series of monocarbonyl curcumin-thiourea/thiazole hybrids as human DNA ligase I (hLigI) inhibitors. These compounds (**14-49**) were synthesized and their antiligase and cytotoxic activities were evaluated *in vitro*. Several compounds from this series have shown significant inhibition of purified hLigI activity and exhibited low micro molar range of cytotoxic activity against one or more cancer cell lines with IC₅₀ values ranging from 1.3-48.8 μM. Among these compound **23**, showed antiligase activity at an IC₅₀ value 24.9±1.8 μM, and selective cytotoxicity against DLD1 cancer cell line (IC₅₀ value 8.7±1.9 μM) compared to the reference curcumin (IC₅₀ values were 51.9±8.7 μM and 33.2±1.8 μM for antiligase and cytotoxic activities against DLD1 cell line respectively) and docking studies showed considerable interactions of compound **23** with hLigI. This new class of potent hLigI inhibitors will serve as a potential lead for further optimization and drug development.

Introduction:

Cancer is an uncontrolled cell division and has the ability to invade other tissues. After cardiovascular diseases, cancer is the most life threatening disease worldwide. There are many targets reported for anticancer drugs and several drugs are available against these targets [1]. But the nonspecific nature of drugs and drug resistance property of cancer cells necessitates the discovery of new targets and new drugs for treatment of cancer [2]. Human DNA ligases are now being tested as attractive new therapeutic targets for the development of novel anticancer drugs [3]. DNA ligases are mainly classified into two families according to their requisite cofactor for ligase-adenylate formation. One is NAD⁺ dependent (essential in eubacteria) and the other is ATP dependent (eukaryotes, viruses, archaea and some eubacteria). [4]. Human DNA ligases fall into ATP-dependent family of ligases which are hLigI, III and IV [5]. The ligases seal

the nick between DNA termini by making phosphodiester bond in a three step reaction mechanism during DNA replication and repair processes [6]. Among these, hLigI plays a major role in DNA replication where it seals the nicks between Okazaki fragments during the lagging strand DNA synthesis and also participates in DNA base excision repair (BER) pathways [7]. Human DNA ligases III and IV play important roles during the DNA repair processes such as BER, Nucleotide excision repair (NER) and Non-homologous end joining pathway (NHEJ) [8].

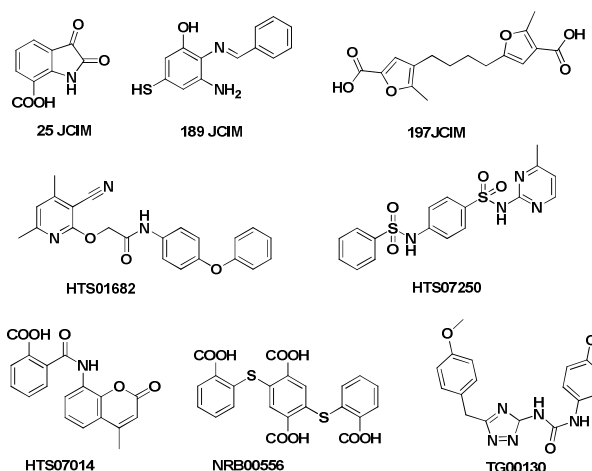


Figure 1. Human DNA Ligase I inhibitors reported in the literature.

^a Medicinal & Process Chemistry Division, CSIR-Central Drug Research Institute (CSIR-CDRI), Jankipuram Extension, Sitapur Road, Lucknow 226031.

^b Molecular & Structural Biology Division, CSIR-Central Drug Research Institute (CSIR-CDRI), Jankipuram Extension, Sitapur Road, Lucknow 226031.

^c Academy of Scientific and Innovative Research (AcSIR), New Delhi-110001 (India).

¹ Present Address: Dept. of Pharmaceutical Chemistry, Global Institute of Pharmaceutical Education and Research, Kashipur, Uttarakhand, 244713, India.

[§]CDRI Communication No: 340/2015/VLS

Electronic Supplementary Information (ESI) available: [Supplementary data like scan copies of ¹H NMR spectral data (compounds **14-49**), ¹³C NMR spectral data (compounds **14-36**, **38-49**) and HRMS spectra (compounds **14-28**, **30-43**, **45-49**) associated with this article can be found in the on-line version.....]. See DOI: 10.1039/x0xx00000x

It has been reported that defects in hLigI promotes aberrant DNA replication, repair and hypersensitivity of cell to DNA damaging agents and immunodeficiency that can promote cellular apoptosis [9]. Due to its participation in such important functions, hLigI has been suggested as a potential new target for some cancers. In 2004, after the discovery of the crystal structure of hLigI-DNA complex [10], it has been gaining a lot of attention for the discovery of novel ligase inhibitors by using computational methods. Although some inhibitors have been identified (Figure 1), none are currently in clinical use [3], making it all the more pertinent to find more potent inhibitors for hLigI that can reach the clinic. Although ligases are expressed in both cancer as well as normal cells, they are reported to be over-expressed in rapidly dividing cancer cells due to which specificity towards cancer cells is expected [11].

Natural products and natural product inspired libraries are the major resources for drug discovery [12]. Classical drug discovery process is a lengthy and expensive process, with low chances of success [13]. To maximize chances of success and limit failures to initial stages, *in silico* approaches are available now. Virtual screening (VS) has become an integral part and an established tool for identification of novel hits. The identification of new chemotypes with the desired biological profile that structurally diverge from known pharmacologically active reference compounds is the principal goal of VS [14]. In the hierarchical VS protocol (this includes ligand-based screening approaches), the first phase deals with the identification of test compounds structurally unrelated to one or a set of known active compounds. This is followed by structure-based virtual screening methods through which molecules that complement the active site of the target protein can be identified [15]. Based on these findings, a pharmacophore based virtual screening approach has been developed for the identification of new chemotypes for the hLigI inhibitors in the present work.

In this study we have screened a library of natural compounds out of which the top 20 have been identified as potential hits to target the hLigI enzymes. These hits were subsequently screened based on docking studies and further analyzed based on their binding energies and affinities towards the target enzyme. The identified curcumin scaffold was used as a template molecule for the design of the series of compounds targeted towards hLigI. These known ligands were taken as template molecules from which a series of 36 novel compounds were designed based on the ligand and structure based approaches to validate our assumptions and subsequently screened for their specific hLigI inhibition and antiproliferative activity.

Hence, in this study we report the identification of a novel class of hLigI inhibitors through an *in silico* approach followed by biological evaluation by enzyme based assays with the purified protein and cell based screening with curcumin as the standard compound. Specific ligase enzyme inhibition studies, MTT assays and apoptosis studies were carried out. A detailed structure activity relationship (SAR) of the compounds in this novel series has also been discussed.

Results and Discussion

Generation and selection of pharmacophore models

The 3D QSAR pharmacophore model generation protocol using 10 training set molecules (Figure 2, a-j) resulted in the development of ten pharmacophore hypotheses. The cost values of the generated hypothesis ranges between (84.746-78.215) indicate good robustness of the models. The first hypothesis Hypo-1 was selected on the basis of mapping of all training set compounds. The Hypo-1 comprising of four features viz., hydrophobic feature (1Z), H-bond acceptor feature (3H) (Figure 3 and Supporting information Table S1). In order to validate this model the Hypo-1 was again used to map the dataset of reported active molecules as hLigI inhibitors. The active compounds from the literature mapped well (Figure 4A) on the developed pharmacophore model and differentiated the least active or moderately active compounds from the dataset. The most active compound from the dataset mapped this model very well, while moderate or least active compounds miss one or more features.

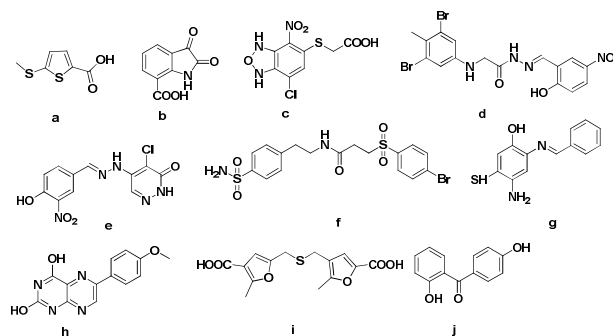


Figure 2. Structures of the 10 most active compounds (a-j) used for the development of pharmacophore model.

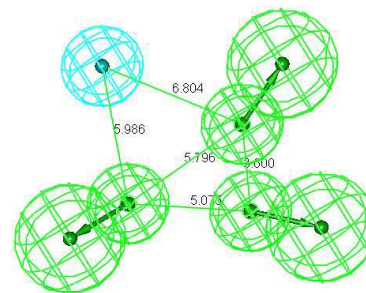


Figure 3. The common feature pharmacophore model generated using 10 diverse compounds.

Pharmacophore complementarities with active site

In order to further validate the complementarities of the pharmacophore model with putative DNA binding site in the DBD of hLigI co-crystallized with DNA (PDB ID: 1X9N) the docking studies were carried out. As a part of internal validation, the docking studies of known active compounds was carried out within this active site. This docking analysis

revealed the most remarkable features of the hLigI inhibitors in active site, which demonstrates the binding modes obtained from the two biologically active molecules (Figure 4B) in the DNA binding region of the catalytic site of DNA ligase I. These ligands also formed hydrogen bond with DNA binding residues including Arg449, Arg451, Gly453, Lys768, and Lys770. The hydrophobic (Z) function of the pharmacophore model is well supported by the hydrophobic interactions within the binding site.

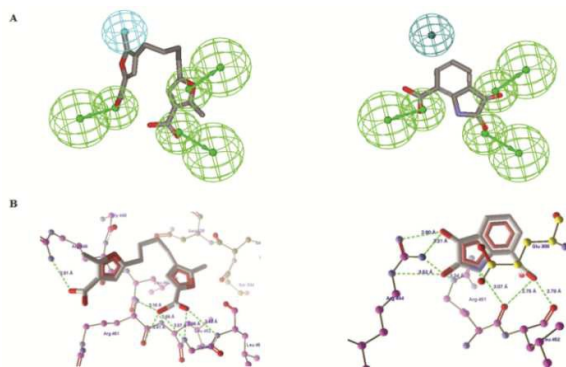


Figure 4. A) Molecular alignments of the reference compounds 197JICM and 25JICM reported as hLigI inhibitors. B) Molecular interactions of 197JICM and 25JICM with important amino acids in the ligand binding domain of the hLigI.

Pharmacophore based virtual screening

In this experiment we carried out our well reported state of the art protocol for virtual screening in which a database of natural compounds was screened against this Hypo-1. The active compound from this database screening curcumin was selected based on ligand pharmacophore mapping, fit values and availability for *in vitro* testing. The mapping showed that 4-hydroxy-3-methoxy group completely maps the two hydrogen bond acceptor features while third acceptor feature was fulfilled by 5-dione group and the hydrophobic feature was supported by the one phenyl ring of curcumin (Figure 5A). On the basis of these observations we further decided to dock the curcumin to validate the ligand based studies. As expected, curcumin was found active with the Moldock and Rerank scores of -122.172 and -93.461 (Fit Value 2.562) with the important hydrogen bond interactions with amino acids Arg449 and Gly453 (Figure 5B). The promising results from both of these studies inspired us to design a novel series of compounds for the hLigI inhibition.

An ideal chemotherapeutic agent would need to inhibit multiple pathways simultaneously, with minimum side effects to normal cells. Curcumin is known to inhibit a number of cell signaling pathways in tumor cells [16]. The metabolic instability of Curcumin is due to the β -diketone moiety. It was replaced with single keto group, to synthesize monocarbonyl curcumin analogues, resulting in improved cytotoxicity and stability [17]. Considering the toxicity and other issues, it was hypothesized to design a novel series of monocarbonyl curcumin-thiourea/thiazole hybrids based on the parent

curcumin structure. A series of 100 compounds was designed from which the top 36 compounds were prioritized for synthesis based on fit value and previously explained docking interactions and the Moldock and Rerank scores (Supporting information Table S2). Out of the top 10 compounds, the most active compound from the series, compound **23**, was predicted to be more active than the rest of the molecules (Supporting information Figure S1). The compound **23** mapped within the pharmacophore model with the fit value of 2.922.

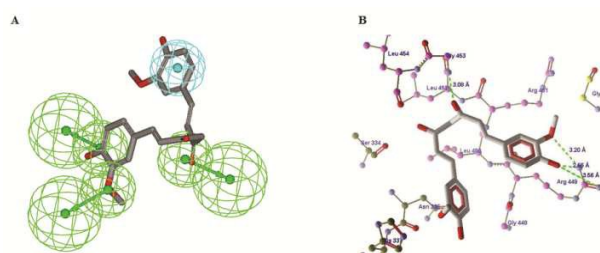
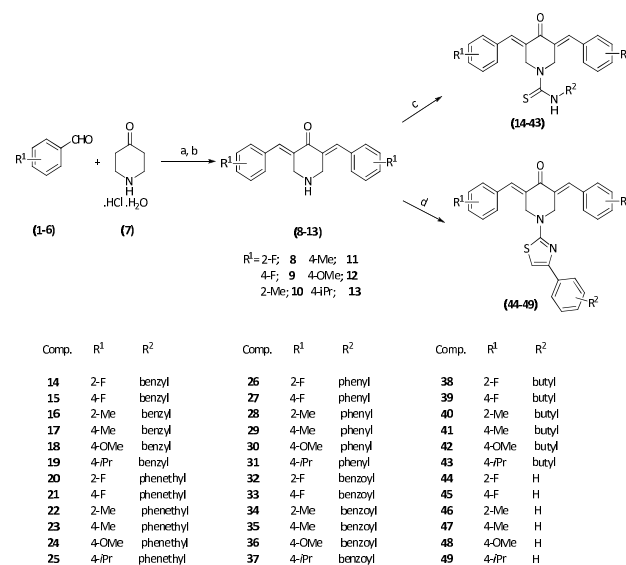


Figure 5. A. Pharmacophore alignments of the curcumin a reference natural compound identified from virtual screening experiment. B. Molecular interactions of curcumin in the DNA binding pocket of hLigI.

Chemistry

The general procedure for the synthesis of the (3E,5E)-N-substituted-3,5-bis(substitutedbenzylidene)-4-oxopiperidine-1-carbothioamide (**14–43**) and (3E,5E)-3,5-bis(substitutedbenzylidene)-1-(4-phenylthiazol-2-yl)piperidin-4-one (**44–49**) has been illustrated in Scheme 1.

Scheme 1.



Reagents and conditions: (a) glacial acetic acid, Conc. HCl, rt, 48 h; (b) K₂CO₃, acetone: water (5:1), 20 °C, 2 h; (c) substituted isothiocyanate (1.1 equiv.), ethanol, rt, 1–1.5 h; (d) phenacyl thiocyanate (1.1 equiv.), ethanol, 80 °C, 8–10 h.

ARTICLE

Journal Name

In the first step, a series of (3E, 5E)-3, 5-bis (substituted benzylidene) piperidin-4-one (**8-13**) were synthesized by the reaction of substituted benzaldehydes (**1-6**) and 4-piperidinone hydrochloride hydrate (**7**) with catalytic amount of conc. HCl in glacial acetic acid. The reaction contents were stirred for 48 hours. Meanwhile a light yellow solid precipitated out which was filtered, and then washed with excess ethyl acetate and air dried. The precipitate obtained was further treated with potassium carbonate in acetone: water (5:1) at room temperature for 2 hours to yield compounds **8-13** (Scheme 1) [21]. Furthermore, compounds **8-13** were reacted with substituted isothiocyanates in ethanol at rt for 1-1.5 hour providing compounds **14-43** in good yields. Subsequent reaction of **8-13** with phenacyl thiocyanate in ethanol at 80°C for 8-10 hour furnished corresponding compounds **44-49** in good yields.

Biological Evaluation

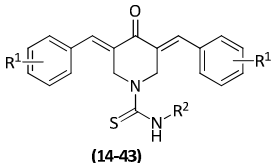
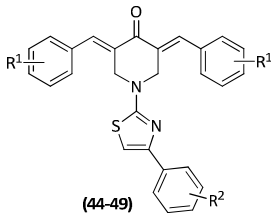
Inhibition of human DNA ligase I activity and cytotoxicity of synthesized compounds

Antiligase activity of monocarbonyl curcumin-thiourea/thiazole hybrids (**14-49**) were evaluated against purified hLigI protein by fluorescence based DNA ligation assay at 50 μM concentration (Table 1). Of these, most potent six compounds (**19, 23, 28, 35, 38** and **30**) showed more than 90% antiligase inhibition while five compounds (**14, 26, 16, 30** and **36**) showed moderate inhibition in the range of 50-75%, and only two compounds (**20** and **39**) showed inhibition of <50%. Rest of the four compounds (**25, 31, 37** and **43**) did not show any inhibitory activity (0%) of hLigI protein. Twenty five compounds (**15, 17-19, 21-24, 27-29, 32-35, 38, 40-42** and **44-49**) exhibited significant antiligase activity (>75% inhibition) against purified hLigI protein at 50 μM concentration while standard curcumin showed 38.6% inhibition at the same concentration. These 25 compounds were further checked for their selective cytotoxic activity in various cancer cell lines.

Structure Activity Relationship (SAR) Study

This study involved two prototypes, monocarbonyl curcumin-thiourea (**14-43**) and monocarbonyl curcumin-thiazole hybrids (**44-49**). The R¹ substituents at phenyl ring of monocarbonyl curcumin moiety were electron withdrawing groups (2-F, 4-F) and electron donating groups (2-Me, 4-Me, 4-OMe, 4-*i*Pr).

Table 1: Percentage inhibition of ligation and cytotoxic activity^a (IC₅₀ in μM) of synthesized compounds (**14-49**).

Comp. No.	% Ligation inhibition at 50 μM	<div style="display: flex; justify-content: space-around; align-items: center;"> <div style="text-align: center;">  <p>(14-43)</p> </div> <div style="text-align: center;">  <p>(44-49)</p> </div> </div>							
		^b DLD1	^c HCT116	^d HT-29	^e HepG2	^f HeLa	^g MDA-MB-231	^h 4T1	ⁱ 3T3
14	65.7±3.1	NT	NT	NT	NT	NT	NT	NT	NT
15	87.4±4.9	> 50	> 50	> 50	> 50	> 50	> 50	> 50	> 50
16	60.4±6.9	NT	NT	NT	NT	NT	NT	NT	NT
17	80.5±3.2	15±1.5	12.2±3.9	11.7±2.3	21.2±0.6	> 50	24.7±4.2	> 50	> 50
18	87.6±8.3	> 50	> 50	> 50	> 50	> 50	> 50	> 50	> 50
19	92.3±6.7	12.1±3.3	> 50	> 50	> 50	39.5±6.7	20.5±2.1	> 50	> 50
20	13.3±9.1	NT	NT	NT	NT	NT	NT	NT	NT
21	85.8±11.1	15.3±4.1	> 50	12.6±1.7	4.8±0.8	34.7±1.4	17.1±2.2	> 50	> 50
22	77.8±3.9	4.9±2.6	> 50	8.1±2.3	14.4±1	> 50	15.9±7.1	> 50	> 50
23	92.3±1.7	8.7±1.9	> 50	> 50	21.2±2.3	> 50	> 50	> 50	40.8±2.1
24	76.4±1.4	26.5±4.2	17.3±4.1	28.5±4.7	> 50	>50	41.9±5.3	> 50	> 50

Journal Name

ARTICLE

25	0	NT	NT	NT	NT	NT	NT	NT	NT
26	69.4±9.1	NT	NT	NT	NT	NT	NT	NT	NT
27	89.9±1.9	> 50	> 50	> 50	> 50	> 50	> 50	> 50	> 50
28	92.7±3.5	> 50	> 50	> 50	> 50	34.2±3.4	13.6±9.1	> 50	> 50
29	83.7±6.7	> 50	> 50	34.4±7.1	16.4±3.2	34.8±3.6	20.5±1.9	21.4±8.8	13.8±3.1
30	71.4±13.3	NT	NT	NT	NT	NT	NT	NT	NT
31	0	NT	NT	NT	NT	NT	NT	NT	NT
32	85.8±9.7	> 50	5.6±3.3	17.5±1.6	21.7±3.9	29.1±1.7	32.6±0.8	18.8±9.1	2.1±1.7
33	77.4±11.9	9.1±5.6	4.5±0.4	> 50	15.5±1.7	31.8±4.3	15.3±3.2	> 50	6.3±4.1
34	96±3.8	> 50	4.2±2.8	11.1±1.8	> 50	> 50	> 50	> 50	> 50
35	93.5±4.3	> 50	9.9±2.1	> 50	12.5±3.4	30.3±6.1	10±4.9	35.6±11.8	> 50
36	57.5±8.4	NT	NT	NT	NT	NT	NT	NT	NT
37	0	NT	NT	NT	NT	NT	NT	NT	NT
38	94.5±2.1	> 50	5.6±4.1	16.4±3.8	> 50	> 50	1.3±0.7	25.3±1.3	2.8±0.9
39	49.8±8.9	NT	NT	NT	NT	NT	NT	NT	NT
40	99.3±0.2	> 50	4.3±1.6	3.6±1.3	11.4±1.4	> 50	> 50	> 50	2.5±1.2
41	82.2±12.8	9.9±3.8	11.6±4.3	27.8±1	> 50	48.8±8.2	25.1±2.9	> 50	0.84±0.2
42	82±3.8	> 50	> 50	> 50	> 50	> 50	> 50	> 50	> 50
43	0	NT	NT	NT	NT	NT	NT	NT	NT
44	90±6.5	> 50	> 50	> 50	> 50	> 50	> 50	> 50	> 50
45	88.5±4.2	> 50	> 50	> 50	> 50	> 50	> 50	> 50	> 50
46	88.3±8.5	16.5±6.1	> 50	> 50	> 50	> 50	40.5±7.2	> 50	> 50
47	87.3±6.7	24.4±1.9	> 50	> 50	> 50	> 50	45.1±4.2	> 50	> 50
48	87.1±7.3	> 50	> 50	> 50	> 50	> 50	> 50	> 50	> 50
49	84.6±8.8	> 50	> 50	> 50	> 50	> 50	> 50	> 50	> 50
Curcumin	38.6±3.7	33.2±1.8	29.7±3.1	39.3±1.5	42.3±1.3	38.3±4.2	36±2.6	50±1.1	34.7±1.9

^aData is represented as mean±SD values from three different experiments, ^{b, c, d} Human Colon cancer cell lines, ^e Human Liver cancer cell line, ^f Human Cervical cancer cell line, ^g breast cancer cell line, ^h Mouse Breast cancer cell line, ⁱ Normal mouse embryonic fibroblast cell line, ^{NT} Not tested as percentage Ligand inhibition at 50 μM was <75%.

The substituents at position R² in the thiourea part were benzyl, phenethyl, phenyl, benzoyl and butyl groups. The hLigI inhibition results suggested that when R¹ was 2-F the activity increased from 13.3% to 94.5% with R² from phenethyl (**20**), benzyl (**14**), phenyl (**26**), benzoyl (**32**), butyl (**38**) while with 4-F at R¹ the increasing order of activity was butyl (**39**) < benzoyl (**33**) < phenethyl (**21**) < benzyl (**15**) < phenyl (**27**) groups at R².

RSC Advances Accepted Manuscript

Published on 02 March 2016. Downloaded by Middle East Technical University (Orta Dogu Teknik U) on 02/03/2016 18:34:03.

ARTICLE

It was inferred that 4-F group at R¹ seemed to be more desirable. Among electron donating substitution at R¹ position 2-Me and 4-Me groups were found to be more suitable as hLigI inhibitory activity was more than 80% in eight compounds (**17**, **23**, **28**, **29**, **34**, **35**, **40**, **41**, **46** and **47**) out of ten. However, 4-OMe and 4-*i*Pr groups were less desirable as only three (**18**, **19** and **42**) out of ten compounds exhibited more than 80% hLigI inhibition. Out of four electron donating groups at R¹ position 4-Me seemed to be most desirable as all the five compounds irrespective of substituents at R² position showed 80.4 to 93.4% inhibition while a 4-*i*Pr group at R¹ position was least favorable as only one compound with benzyl at R² was active (**19**, 92.3%) and rest were inactive. All the thiazole hybrids (**44**–**49**) exhibited significant hLigI inhibition (84.6–89.9%) with both the electron withdrawing (2-F, 4-F) and electron donating (2-Me, 4-Me, 4-OMe, 4-*i*Pr) substituents at R¹ position. Therefore the SAR study revealed that the hybridization of monocarbonyl curcumin with thiourea (**14**–**43**) was more suited for hLigI inhibition as several compounds exhibited more than 90% inhibitory activity.

With the emergence of human DNA ligase as attractive target for the development of new anticancer compounds, it was thought worthwhile to study the *in vitro* cytotoxic activity of hybrid molecules showing significant inhibition (>75%) of DNA ligase I activity. The compounds were screened against different cancer cell lines, such as DLD1, HCT116, HT-29 (human colon cancer), 4T1 (mouse breast cancer), MDA-MB-231 (human breast cancer), HepG2 (human liver cancer), and HeLa (human cervical cancer) by MTT assay. The results were summarized in Table 1 along with curcumin as a reference standard. Of all the twenty five compounds tested, seventeen compounds (**17**, **19**, **21**–**24**, **28**, **29**, **32**–**35**, **38**, **40**, **41**, **46** and **47**) showed cytotoxic activity against more than one cancer cell line with IC₅₀ values 1.3–48.8 μM (Table 1) whereas standard curcumin exhibited IC₅₀ of 29.7–50 μM in five cancer cell lines. The selective cytotoxicity data suggested that monocarbonyl curcumin-thiourea hybrids were more desirable over monocarbonyl curcumin-thiazole hybrids as in case of hLigI inhibitory activity. Most of the compounds were found to be safe against normal mouse embryonic fibroblast cell line (3T3). Seventeen compounds (**17**, **19**, **21**–**24**, **28**, **29**, **32**–**35**, **38**, **40**, **41**, **46** and **47**) showed both the antiligase as well as cytotoxic activity in different cancer cell lines much more potent than that of parent curcumin. Compound **23** was chosen for further mechanistic studies due to its high antiligase activity against purified hLigI protein and high cytotoxic activity against colon cancer cell line (DLD1) and its low toxicity against the normal cell line (3T3).

Antiligase activity and induced morphological changes in DLD 1 cells treated with compound 23

Antiligase activity of compound **23** and curcumin (Figure 6A) were performed at different concentration (6.3, 12.5, 25, 50, 100 μM) and the IC₅₀ values were calculated. It was found that compound **23** inhibits ligation at lower IC₅₀ value (24.9±1.8 μM) as compared to curcumin (51.9±8.7 μM). The graph in

Figure 6A shows percent ligation inhibition by compound **23** as compared to curcumin.

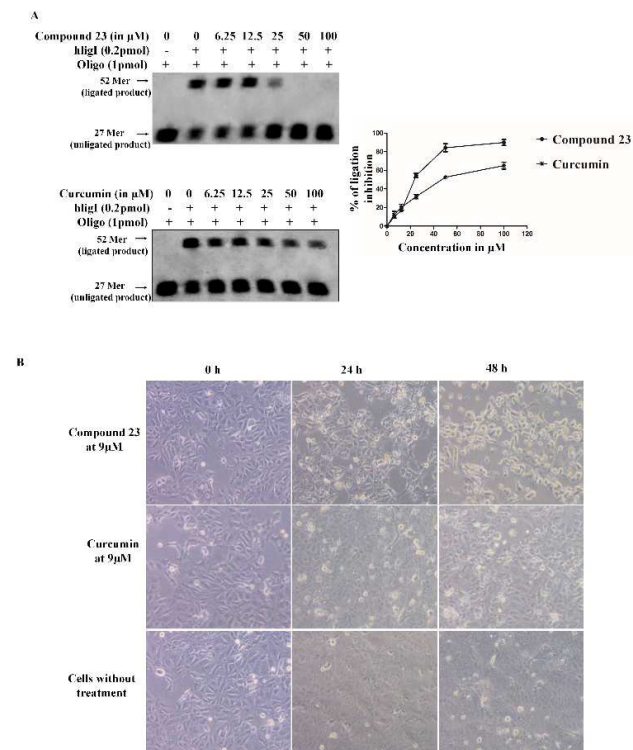


Figure 6. A. Gel images for ligation assay and % ligation inhibition of compound **23** and curcumin at different doses. B. Bright field images of treated (compound **23** and curcumin) and DMSO treated DLD1 cells.

Differences in cell morphology were observed among compound **23**, curcumin and vehicle treated cells by light microscopy. The cells were treated with 9 μM concentration of either compound **23** or curcumin for different time intervals (0, 24, and 48 h.). As shown in Figure 6B, it was observed that compound **23** induced the most conspicuous morphological changes in DLD1 cells as compared to curcumin and untreated cells. The morphological changes included cell shrinkage and extensive detachment of cells from the cell culture substratum, which are characteristics of apoptotic cell death [18]. The morphological changes became more prominent with increases in drug concentration and time of drug treatment.

Compound 23 inhibits ligation by abolishing the interaction between hLigI and DNA

A compound can inhibit DNA ligase activity mainly by two methods. One is by direct interaction with the ligase protein and the second is by interaction with the DNA to indirectly occlude protein binding. To examine whether the compound **23** interacts with the DNA or the protein, gel retardation assay, DNase I cleavage protection assay (for the study of interaction between compound and DNA) and electrophoretic mobility

shift assay (EMSA) (for the study of interaction between compound and protein) were performed.

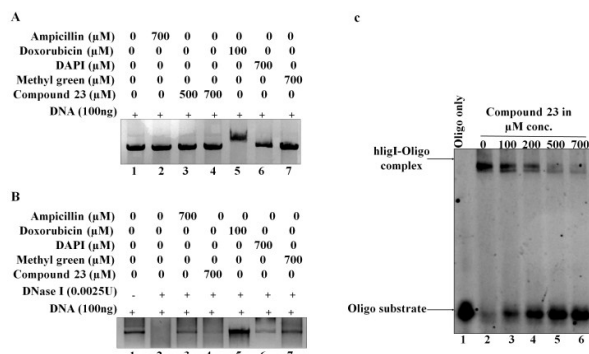


Figure 7. A. Gel retardation assay performed for compound **23** with various controls. Compound **23** (lanes 3, 4) did not show any gel retardation. B. DNase I protection assay for compound **23** with various controls. Compound **23** did not offer protection to DNA from DNase digestion. C. Electrophoretic Mobility Shift Assay (EMSA) for compound **23** with DNA and protein shows competitive inhibition of DNA-protein complex formation in the presence of compound **23** (lanes 3-6 compared to lane 2).

In the gel retardation assay (Figure 7A), unlike doxorubicin (DNA intercalator) and DAPI (DNA minor groove binder), there was no hindrance seen in the movement of DNA in an agarose gel in the presence of compound **23** even up to 700 μM concentration (Figure 7A, lane 3, 4 versus lane 5 and 6). However, in this experiment there was no hindrance seen in the movement of DNA incubated with methyl green as well (DNA major groove binder). We therefore also performed a DNase I cleavage protection assay (Figure 7B), which reveals that unlike the doxorubicin, DAPI and methyl green (all three are DNA binders) the DNA incubated with compound **23** was completely cleaved with DNase I (Lane 4 versus lane 5-7 in Figure 7B). Therefore, we conclude from our gel based experiments that compound **23** most probably doesn't interact with DNA. In the EMSA assay (Figure 7C), increasing concentrations of compound **23** (100, 200, 500, 700 μM) reduced the interaction between hLigI and nicked DNA substrate. This reduction in interaction between hLigI and DNA (Figure 7C, lane 2 versus lane 3-6) indicates that compound **23** interacts with either the protein or the protein-DNA complex in such a way that the protein can no longer bind to DNA and results in inhibition of ligation by competitive mode of inhibition.

Flow cytometry and Western blotting analysis

Flow cytometry analysis suggested that compound **23** significantly induced apoptotic death of DLD1 cells at IC₅₀ concentration of 9 μM. It showed 12.0±2.1% and 29.7±4.2% of apoptotic cell death at 4.5 and 9 μM concentrations for 48 h of treatment respectively (Figure 8A). In the treated cells we

checked the expression level of γH2AX which acts as biomarker for DNA strand breaks [19]. The increased level of γH2AX showed that the compound **23** increases instances of double strand DNA breaks in the cell leading to increased genomic instability. A decrease was also observed in the expression level of proliferating cell nuclear antigen (PCNA) which serves as the cell proliferation marker [20]. The decreased expression of PCNA in the presence of compound **23** in DLD1 cells reveals that the compound inhibits the cell proliferation and promotes the cell death towards apoptosis (Figure 8B).

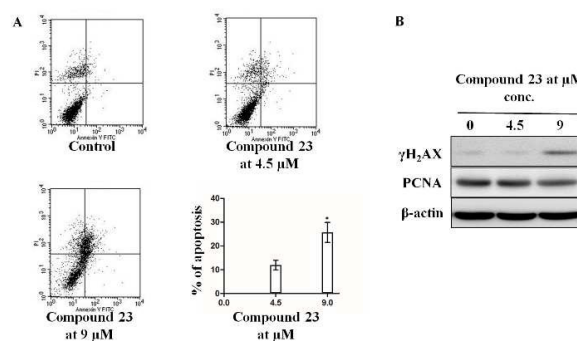


Figure 8. A. DLD1 cells were treated with different concentrations (0, 4.5, 9 μM) of compound **23** for 48 h. The percentages of cells undergoing apoptosis at different concentrations of the inhibitor are represented graphically. B. Expression level of γH2AX and PCNA was increased in DLD1 cells treated with compound **23**.

Docking analysis

The mode of binding of the compounds (**14-49**) with target protein hLigI was analyzed by the Molegro virtual docker 4.0 and the visualizer 3.0 in Discovery studio. In order to validate the docking protocol, the reference compound curcumin and the active molecule in this study were docked in the DNA binding site of the hLigI. The docking interactions of these ligands at the binding site showed a similar binding pattern with the binding site residues reported to be important, as shown by their scoring functions (Supplementary Table S2). In this experiment the compounds showed good binding affinity and selectivity towards hLigI as compared to the reference molecules curcumin. The docking study clearly supports the observation that these compounds inhibit the hLigI activity (the comparative docking scores are represented in the supplementary Table S2). The top 36 compounds obtained by pharmacophore mapping were subjected to docking into the active site of hLigI. Table S2 shows scoring functions as an output of these docking experiments and the top scoring compound **23** from both pharmacophore and docking runs was analyzed for its binding modes within the active site (Figure 9). Compound **23** showed comparatively higher binding affinities represented by Moldock and Reranks scores respectively at lower IC₅₀ values. To further validate these results the molecular interactions of all the molecules at receptor binding site were studied (Supporting Figure S1). The compound **23** showed higher binding interactions at the active

ARTICLE

Journal Name

site of hLigI protein (in PDB 1X9N) with the amino acids viz., His337, Arg449, Arg451 and Gly453 that are located in the DBD region.

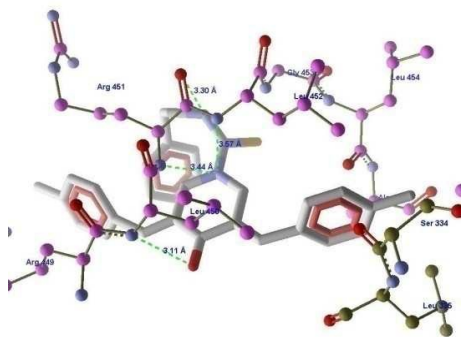


Figure 9. Ligand protein interactions of the highly active compound **23** within the DNA binding domain of the hLigI.

Conclusions

DNA replication and repair are indispensable processes for cell survival in both normal as well as cancerous cells. Faster growth leads to elevated levels of ligase proteins in cancer cells making them potential therapeutic targets for cancer chemotherapy, at least in some cancers [11]. In this study we have generated a 3D-QSAR pharmacophore model for the designing of a novel class of (3E,5E)-N-substituted-3,5-bis(substitutedbenzylidene)-4-oxopiperidine-1-carbothioamide (**14-43**) and (3E,5E)-3,5-bis(substitutedbenzylidene)-1-(4-phenylthiazol-2-yl)piperidin-4-one (**44-49**) compounds as hLigI inhibitors. This pharmacophore model was validated using some already reported ligase inhibitors. Further, the complementarity of the developed pharmacophore model was validated by using docking studies and thirty six compounds were synthesized.

Initially, antiligase activity of all the synthesized compounds was tested against hLigI protein and interestingly twenty five compounds (**15**, **17-19**, **21-24**, **27-29**, **32-35**, **38**, **40-42** and **44-49**) significantly inhibited hLigI activity (>75%) at 50 μ M concentration. Further, these compounds exhibited potent anti-cancer activity against seven cancer cell lines, DLD1, HCT116, MDA-MB-231, HT-29, HepG2, HeLa and 4T1 at 50 μ M concentrations. Of these, seventeen compounds (**17**, **19**, **21-24**, **28**, **29**, **32-35**, **38**, **40**, **41**, **46** and **47**) inhibited proliferation of two or more types of tested cancer cells with IC_{50} values of 1.3-48.8 μ M. The active compound **23** showed better inhibition of purified hLigI and antiproliferative activity as compared to standard curcumin (Figure 6 and Table 1). Compound **23** inhibited DNA ligation by abolishing the interaction between hLigI and DNA. Compound **23** reduced the expression of PCNA and increased the expression of γ H2AX and PARP cleavage in DLD1 cells. This indicates that the compound increases genomic instability and apoptotic cell death in DLD1 cells. Molecular docking studies indicate considerable interactions at the active site of hLigI with the same amino

acids that are located in the DBD domain and involved in DNA binding.

In summary, the present study describes a novel class of hLigI inhibitors with selective cytotoxic activity against cancer cells. The promising biological activity of the synthesized compounds may be a useful starting point for further structural modifications using different medicinal chemistry tools. Further lead optimization studies are in progress and will be reported in the future.

Experimental Section

Chemistry

In general, all reagents and solvents were of research quality and were used without further purification. Chromatography was performed on silica gel (100-200 and 60-120 mesh). All reactions were monitored by thin-layer chromatography (TLC) using F254 silica gel plates with fluorescence (Aldrich). Melting points were determined in open capillary tubes on an electrically heated block and are uncorrected. IR spectra (ν_{\max} in cm^{-1}) of the compounds were recorded on Perkin Elmer FT-IR RX1 PC spectrophotometer. NMR spectra were recorded on Bruker Supercon Magnet Avance DPX-200/DRX-300 spectrometers (operating at 400 and 100 MHz, respectively, for ^1H and ^{13}C) in deuterated solvents with TMS as internal reference (chemical shifts δ in ppm, J in Hz.). Electrospray ionization mass spectra (ESI-MS) were recorded on Ion Trap LCQ Advantage Max-IT (Thermo Electron Corporation). High-resolution mass spectra (HRMS) were recorded on a 6520 Agilent Q ToF LC MS/MS (accurate mass). Elemental analyses were performed on a Carlo Erba EA-1108 micro analyzer / Vario EL-III C, H, N analyzer. All compounds were analyzed for C, H, N and the results obtained were within $\pm 0.4\%$ of calculated values. All final compounds were found to have >95% purity.

Compounds **8-13** ((3E, 5E)-3, 5-bis (substitutedbenzylidene) piperidin-4-one) were synthesized according to an earlier reported procedure [19].

(3E,5E)-N-benzyl-3,5-bis(2-fluorobenzylidene)-4-oxopiperidine-1-carbothioamide (**14**)

The title compound was synthesized from (3E,5E)-3,5-bis(2-fluorobenzylidene)piperidin-4-one (**8**) and benzyl isothiocyanate in 91% yield as yellow solid. mp: 164-166 $^{\circ}\text{C}$; IR (KBr) ν (cm^{-1}): 3410, 1639, 1402, 1216, 771; ^1H NMR (400 MHz, CDCl_3): δ 7.88 (s, 2H), 7.41–7.31 (m, 5H), 7.27–7.26 (m, 2H), 7.20–7.16 (m, 2H), 7.13–7.08 (m, 4H), 5.38 (s, 1H), 4.98 (s, 4H), 4.68 (d, J = 3.0, 2H); ^{13}C (100 MHz, CDCl_3): δ 186.1, 182.3, 161.8, 159.3, 137.2, 133.0, 131.6, 131.5, 131.2, 131.1, 130.7, 128.7, 127.7, 127.6, 124.4, 124.4, 122.1, 122.0, 116.2, 116.0, 50.5, 49.0, 48.9; ESI-MS: m/z 461 ($\text{M}+\text{H}^+$); HRMS (ESI): m/z calculated for $\text{C}_{27}\text{H}_{22}\text{F}_2\text{N}_2\text{OS}$ + H^+ ($\text{M}+\text{H}^+$): 461.1499. Found: 461.1498. Elemental analysis (%) for $\text{C}_{27}\text{H}_{22}\text{F}_2\text{N}_2\text{OS}$: Calcd.: C, 70.42; H, 4.81; N, 6.08; Found, C, 70.64; H, 4.50; N, 5.88.

(3E,5E)-N-benzyl-3,5-bis(4-fluorobenzylidene)-4-oxopiperidine-1-carbothioamide (**15**)

The title compound was synthesized from (3E,5E)-3,5-bis(4-fluorobenzylidene)piperidin-4-one (**9**) and benzyl isothiocyanate in 86% yield as yellow solid. mp: 176–178 °C; IR (KBr) ν (cm⁻¹): 3412, 1640, 1216, 840; ¹H NMR (400 MHz, CDCl₃): δ 7.78 (s, 2H), 7.38–7.35 (m, 4H), 7.29–7.23 (m, 3H), 7.11–7.05 (m, 6H), 5.27 (s, 1H), 5.07 (d, *J* = 0.8, 4H), 4.65 (d, *J* = 4.6, 2H); ¹³C (100 MHz, CDCl₃+DMSO-*d*₆): δ 187.2, 182.7, 164.2, 161.7, 138.3, 136.2, 132.6, 132.5, 131.3, 130.5, 128.2, 127.2, 127.0, 115.9, 115.6, 49.8, 48.5; ESI-MS: *m/z* 461 (M+H⁺); HRMS (ESI): *m/z* calculated for C₂₇H₂₂F₂N₂OS + H⁺ (M+H⁺): 461.1499. Found: 461.1498. Elemental analysis (%) for C₂₇H₂₂F₂N₂OS: Calcd.: C, 70.42; H, 4.81; N, 6.08; Found, C, 70.13; H, 5.09; N, 6.38.

(3E,5E)-N-benzyl-3,5-bis(2-methylbenzylidene)-4-oxopiperidine-1-carbothioamide (16)

The title compound was synthesized from (3E,5E)-3,5-bis(2-methylbenzylidene)piperidin-4-one (**10**) and benzyl isothiocyanate in 85% yield as yellow solid. mp: 164–166 °C; IR (KBr) ν (cm⁻¹): 3409, 3019, 1639, 1402, 1384, 1215; ¹H NMR (400 MHz, CDCl₃): δ 7.99 (s, 2H), 7.28–7.19 (m, 11H), 7.06–7.03 (m, 2H), 5.16 (s, 1H), 4.94 (d, *J* = 1.48 Hz, 4H), 4.64 (d, *J* = 4.76 Hz, 2H), 2.30 (s, 6H); ¹³C (100 MHz, CDCl₃): δ 187.1, 181.9, 138.1, 137.6, 137.2, 133.1, 131.7, 130.6, 129.6, 128.8, 128.7, 127.6, 125.9, 50.5, 48.7, 20.0; ESI-MS: *m/z* 453 (M+H⁺); HRMS (ESI): *m/z* calculated for C₂₉H₂₈N₂OS + H⁺ (M+H⁺): 453.2001. Found: 453.2001. Elemental analysis (%) for C₂₉H₂₈N₂OS: Calcd.: C, 76.96; H, 6.24; N, 6.19; Found, C, 76.80; H, 6.01; N, 6.47.

(3E,5E)-N-benzyl-3,5-bis(4-methylbenzylidene)-4-oxopiperidine-1-carbothioamide (17)

The title compound was synthesized from (3E,5E)-3,5-bis(4-methylbenzylidene)piperidin-4-one (**11**) and benzyl isothiocyanate in 88% yield as yellow solid. mp: 200–202 °C; IR (KBr) ν (cm⁻¹): 3410, 3022, 1615, 1384, 1219; ¹H NMR (400 MHz, CDCl₃): δ 7.81 (s, 2H), 7.30–7.28 (m, 5H), 7.24–7.20 (m, 6H), 7.03 (d, *J* = 6.3 Hz, 2H), 5.29 (s, 1H), 5.11 (s, 4H), 4.65 (d, *J* = 4.7 Hz, 2H), 2.40 (s, 6H); ¹³C (100 MHz, DMSO-*d*₆): δ 187.1, 183.1, 139.9, 139.7, 136.6, 132.2, 132.1, 131.2, 129.8, 128.5, 127.2, 126.9, 49.2, 49.1, 21.5; ESI-MS: *m/z* 453 (M+H⁺); HRMS (ESI): *m/z* calculated for C₂₉H₂₈N₂OS + H⁺ (M+H⁺): 453.2001. Found: 453.2003. Elemental analysis (%) for C₂₉H₂₈N₂OS: Calcd.: C, 76.96; H, 6.24; N, 6.19; Found, C, 76.66; H, 6.42; N, 6.02.

(3E,5E)-N-benzyl-3,5-bis(4-methoxybenzylidene)-4-oxopiperidine-1-carbothioamide (18)

The title compound was synthesized from (3E,5E)-3,5-bis(4-methoxybenzylidene)piperidin-4-one (**12**) and benzyl isothiocyanate in 84% yield as yellow solid. mp: 212–214 °C; IR (KBr) ν (cm⁻¹): 3413, 1630, 1385, 1216, 1069; ¹H NMR (400 MHz, CDCl₃): δ 7.78 (s, 2H), 7.36 (d, *J* = 8.7, 4H), 7.24–7.22 (m, 3H), 7.05–7.03 (m, 2H), 6.92 (d, *J* = 8.8, 4H), 5.31 (s, 1H), 5.11 (d, *J* = 1.1, 4H), 4.66 (d, *J* = 4.7, 2H), 3.86 (s, 6H); ¹³C (100 MHz, CDCl₃+DMSO-*d*₆): δ 191.8, 187.7, 165.4, 144.0, 141.3, 137.5, 134.9, 133.0, 132.0, 131.9, 131.6, 119.1, 60.2, 54.3, 53.8; ESI-MS: *m/z* 485 (M+H⁺); HRMS (ESI): *m/z* calculated for C₂₉H₂₈N₂O₃S + H⁺ (M+H⁺): 485.1899. Found: 485.1897.

Elemental analysis (%) for C₂₉H₂₈N₂O₃S: Calcd.: C, 71.87; H, 5.82; N, 5.78; Found, C, 71.74; H, 5.49; N, 5.96.

(3E,5E)-N-benzyl-3,5-bis(4-isopropylbenzylidene)-4-oxopiperidine-1-carbothioamide (19)

The title compound was synthesized from (3E,5E)-3,5-bis(4-isopropylbenzylidene)piperidin-4-one (**13**) and benzyl isothiocyanate in 80% yield as yellow solid. mp: 188–190 °C; IR (KBr) ν (cm⁻¹): 3411, 3019, 1618, 1385, 1215; ¹H NMR (400 MHz, CDCl₃): δ 7.84 (s, 2H), 7.34 (d, *J* = 8.1 Hz, 4H), 7.29–7.27 (m, 5H), 7.25–7.23 (m, 2H), 7.08–7.06 (m, 2H), 5.33 (s, 1H), 5.13 (d, *J* = 1.4 Hz, 4H), 4.68 (d, *J* = 4.8 Hz, 2H), 3.00–2.90 (m, 2H), 1.29 (d, *J* = 6.9 Hz, 12H); ¹³C (100 MHz, CDCl₃): δ 187.0, 182.3, 150.9, 138.2, 137.3, 131.7, 130.7, 130.5, 128.6, 127.6, 127.5, 127.0, 50.4, 49.0, 34.0, 23.7; ESI-MS: *m/z* 509 (M+H⁺); HRMS (ESI): *m/z* calculated for C₃₃H₃₆N₂OS + H⁺ (M+H⁺): 509.2627. Found: 509.2626. Elemental analysis (%) for C₃₃H₃₆N₂OS: Calcd.: C, 77.91; H, 7.13; N, 5.51; Found, C, 77.65; H, 7.35; N, 5.72.

(3E,5E)-3,5-bis(2-fluorobenzylidene)-4-oxo-N-phenethylpiperidine-1-carbothioamide (20)

The title compound was synthesized from (3E,5E)-3,5-bis(2-fluorobenzylidene)piperidin-4-one (**8**) and phenethyl isothiocyanate in 77% yield as yellow solid. mp: 146–148 °C; IR (KBr) ν (cm⁻¹): 3412, 1632, 1384, 1215, 758; ¹H NMR (400 MHz, CDCl₃): δ 7.88 (s, 2H), 7.47–7.42 (m, 2H), 7.38–7.34 (m, 2H), 7.23–7.16 (m, 7H), 7.02–6.99 (m, 2H), 5.24 (s, 1H), 4.90 (s, 4H), 3.77 (q, *J*₁ = 6.7 Hz, *J*₂ = 11.9 Hz, 2H), 2.76 (t, *J* = 6.8 Hz, 2H); ¹³C (100 MHz, CDCl₃+DMSO-*d*₆): δ 191.1, 188.1, 166.8, 164.8, 145.4, 138.0, 136.3, 136.3, 135.7, 134.6, 134.5, 133.5, 133.2, 130.1, 130.0, 129.1, 127.3, 127.1, 120.7, 120.5, 54.4, 53.4, 39.7; ESI-MS: *m/z* 475 (M+H⁺); HRMS (ESI): *m/z* calculated for C₂₈H₂₄F₂N₂OS + H⁺ (M+H⁺): 475.1656. Found: 475.1655. Elemental analysis (%) for C₂₈H₂₄F₂N₂OS: Calcd.: C, 70.86; H, 5.10; N, 5.90; Found, C, 70.70; H, 5.45; N, 5.78.

(3E,5E)-3,5-bis(4-fluorobenzylidene)-4-oxo-N-phenethylpiperidine-1-carbothioamide (21)

The title compound was synthesized from (3E,5E)-3,5-bis(4-fluorobenzylidene)piperidin-4-one (**9**) and phenethyl isothiocyanate in 88% yield as yellow solid. mp: 184–186 °C; IR (KBr) ν (cm⁻¹): 3410, 1640, 1215, 760; ¹H NMR (400 MHz, CDCl₃): δ 7.77 (s, 2H), 7.41–7.37 (m, 4H), 7.23–7.21 (m, 3H), 7.18–7.14 (m, 4H), 7.01–6.99 (m, 2H), 5.19 (s, 1H), 4.99 (s, 4H), 3.78 (q, *J*₁ = 6.4 Hz, *J*₂ = 11.8 Hz, 2H), 2.77 (t, *J* = 6.6 Hz, 2H); ¹³C (100 MHz, CDCl₃+DMSO-*d*₆): δ 191.9, 187.0, 169.0, 166.5, 144.2, 140.6, 137.7, 137.6, 136.5, 136.4, 135.7, 135.6, 133.5, 133.5, 133.1, 133.1, 130.9, 120.8, 120.5, 53.2, 52.2, 39.7; ESI-MS: *m/z* 475 (M+H⁺); HRMS (ESI): *m/z* calculated for C₂₈H₂₄F₂N₂OS + H⁺ (M+H⁺): 475.1656. Found: 475.1655. Elemental analysis (%) for C₂₈H₂₄F₂N₂OS: Calcd.: C, 70.86; H, 5.10; N, 5.90; Found, C, 70.50; H, 5.22; N, 6.10.

(3E,5E)-3,5-bis(2-methylbenzylidene)-4-oxo-N-phenethylpiperidine-1-carbothioamide (22)

The title compound was synthesized from (3E,5E)-3,5-bis(2-methylbenzylidene)piperidin-4-one (**10**) and phenethyl isothiocyanate in 80% yield as yellow solid. mp: 106–108 °C; IR (KBr) ν (cm⁻¹): 3413, 3019, 2400, 1618, 1523, 1215; ¹H NMR (400 MHz, CDCl₃): δ 7.99 (s, 2H), 7.35–7.27 (m, 7H), 7.20 (d, *J* =

ARTICLE

Journal Name

7.0 Hz, 4H), 6.95–6.92 (m, 2H), 5.05 (s, 1H), 4.85 (d, $J = 1.3$ Hz, 4H), 3.72 (q, $J_1 = 6.9$ Hz, $J_2 = 11.9$, 2H), 2.67 (d, $J = 6.8$ Hz, 2H), 2.38 (s, 6H); ^{13}C (100 MHz, CDCl_3): δ 187.2, 181.9, 138.3, 138.2, 137.5, 133.3, 131.6, 130.6, 129.6, 128.9, 128.6, 128.4, 126.5, 126.0, 48.3, 47.2, 34.7, 20.1; ESI-MS: m/z 467 ($\text{M}+\text{H}^+$); HRMS (ESI): m/z calculated for $\text{C}_{30}\text{H}_{30}\text{N}_2\text{O}_5\text{S} + \text{H}^+$ ($\text{M}+\text{H}^+$): 467.2157. Found: 467.2158. Elemental analysis (%) for $\text{C}_{30}\text{H}_{30}\text{N}_2\text{O}_5\text{S}$: Calcd.: C, 77.22; H, 6.48; N, 6.00; Found, C, 77.50; H, 6.81; N, 6.11.

(3E,5E)-3,5-bis(4-methylbenzylidene)-4-oxo-N-phenethylpiperidine-1-carbothioamide (23)

The title compound was synthesized from (3E,5E)-3,5-bis(4-methylbenzylidene)piperidin-4-one (**11**) and phenethyl isothiocyanate in 79% yield as yellow solid. mp: 182–184 °C; IR (KBr) ν (cm^{-1}): 3415, 3015, 1619, 1511, 1215; ^1H NMR (400 MHz, CDCl_3): δ 7.80 (s, 2H), 7.33–7.27 (m, 8H), 7.21–7.19 (m, 3H), 6.97–6.95 (m, 2H), 5.17 (s, 1H), 5.03 (d, $J = 1.3$ Hz, 4H), 3.73 (q, $J_1 = 6.8$ Hz, $J_2 = 11.8$ Hz, 2H), 2.70 (t, $J = 6.8$ Hz, 2H), 2.43 (s, 6H); ^{13}C (100 MHz, $\text{DMSO}-d_6$): δ 187.1, 182.2, 139.9, 139.8, 136.4, 132.1, 131.3, 129.9, 129.0, 128.7, 126.4, 48.9, 47.5, 34.9, 21.5; ESI-MS: m/z 467 ($\text{M}+\text{H}^+$); HRMS (ESI): m/z calculated for $\text{C}_{30}\text{H}_{30}\text{N}_2\text{O}_5\text{S} + \text{H}^+$ ($\text{M}+\text{H}^+$): 467.2157. Found: 467.2157. Elemental analysis (%) for $\text{C}_{30}\text{H}_{30}\text{N}_2\text{O}_5\text{S}$: Calcd.: C, 77.22; H, 6.48; N, 6.00; Found, C, 77.49; H, 6.28; N, 6.36.

(3E,5E)-3,5-bis(4-methoxybenzylidene)-4-oxo-N-phenethylpiperidine-1-carbothioamide (24)

The title compound was synthesized from (3E,5E)-3,5-bis(4-fluorobenzylidene)piperidin-4-one (**12**) and phenethyl isothiocyanate in 85% yield as yellow solid. mp: 162–164 °C; IR (KBr) ν (cm^{-1}): 3412, 1636, 1384, 1215, 1069; ^1H NMR (400 MHz, CDCl_3): δ 7.78 (s, 2H), 7.38 (d, $J = 8.7$ Hz, 4H), 7.23–7.19 (m, 3H), 6.99 (d, $J = 8.7$ Hz, 6H), 5.20 (s, 1H), 5.03 (d, $J = 1.3$ Hz, 4H), 3.89 (s, 6H), 3.79–3.74 (m, 2H), 2.73 (t, $J = 6.7$ Hz, 2H); ^{13}C (100 MHz, $\text{DMSO}-d_6$): δ 186.8, 182.2, 160.7, 139.8, 136.1, 133.2, 130.7, 129.0, 128.7, 127.5, 126.4, 114.8, 55.8, 48.8, 47.6, 35.0; ESI-MS: m/z 499 ($\text{M}+\text{H}^+$); HRMS (ESI): m/z calculated for $\text{C}_{30}\text{H}_{30}\text{N}_2\text{O}_5\text{S} + \text{H}^+$ ($\text{M}+\text{H}^+$): 499.2055. Found: 499.2052. Elemental analysis (%) for $\text{C}_{30}\text{H}_{30}\text{N}_2\text{O}_5\text{S}$: Calcd.: C, 72.26; H, 6.06; N, 5.62; Found, C, 72.01; H, 6.34; N, 5.92.

(3E,5E)-3,5-bis(4-isopropylbenzylidene)-4-oxo-N-phenethylpiperidine-1-carbothioamide (25)

The title compound was synthesized from (3E,5E)-3,5-bis(4-isopropylbenzylidene)piperidin-4-one (**13**) and phenethyl isothiocyanate in 85% yield as yellow solid. mp: 144–146 °C; IR (KBr) ν (cm^{-1}): 3409, 3019, 1613, 1524, 1216; ^1H NMR (400 MHz, CDCl_3): δ 7.81 (s, 2H), 7.38–7.33 (m, 8H), 7.21–7.19 (m, 3H), 6.99–6.96 (m, 2H), 5.16 (s, 1H), 5.05 (s, 4H), 3.73 (q, $J_1 = 6.8$ Hz, $J_2 = 11.9$ Hz, 2H), 3.04–2.94 (m, 2H), 2.68 (t, $J = 6.8$ Hz, 2H), 1.31 (d, $J = 6.9$ Hz, 12H); ^{13}C (100 MHz, $\text{DMSO}-d_6$): δ 187.0, 182.2, 151.0, 138.5, 138.0, 131.9, 130.7, 130.6, 128.6, 128.5, 127.1, 126.5, 48.8, 47.2, 34.7, 34.0, 23.7; ESI-MS: m/z 523 ($\text{M}+\text{H}^+$); HRMS (ESI): m/z calculated for $\text{C}_{34}\text{H}_{38}\text{N}_2\text{O}_5\text{S} + \text{H}^+$ ($\text{M}+\text{H}^+$): 523.2783. Found: 523.2778. Elemental analysis (%) for $\text{C}_{34}\text{H}_{38}\text{N}_2\text{O}_5\text{S}$: Calcd.: C, 78.12; H, 7.33; N, 5.36; Found, C, 78.00; H, 7.52; N, 5.63.

(3E,5E)-3,5-bis(2-fluorobenzylidene)-4-oxo-N-phenethylpiperidine-1-carbothioamide (26)

The title compound was synthesized from (3E,5E)-3,5-bis(2-fluorobenzylidene)piperidin-4-one (**8**) and phenyl isothiocyanate in 83% yield as yellow solid. mp: 176–178 °C; IR (KBr) ν (cm^{-1}): 3409, 1630, 1385, 1215, 757; ^1H NMR (400 MHz, CDCl_3): δ 7.91 (s, 2H), 7.43–7.37 (m, 2H), 7.28–7.11 (m, 9H), 7.05–7.01 (m, 1H), 6.93 (d, $J = 7.5$, 2H), 4.95 (s, 4H); ^{13}C (100 MHz, $\text{CDCl}_3+\text{DMSO}-d_6$): δ 191.0, 188.0, 167.0, 164.5, 145.5, 138.1, 136.4, 136.3, 135.8, 134.4, 133.1, 130.2, 130.0, 129.2, 127.3, 127.2, 120.7, 120.5, 54.4; ESI-MS: m/z 447 ($\text{M}+\text{H}^+$); HRMS (ESI): m/z calculated for $\text{C}_{26}\text{H}_{20}\text{F}_2\text{N}_2\text{O}_5\text{S} + \text{H}^+$ ($\text{M}+\text{H}^+$): 447.1343. Found: 447.1356. Elemental analysis (%) for $\text{C}_{26}\text{H}_{20}\text{F}_2\text{N}_2\text{O}_5\text{S}$: Calcd.: C, 69.94; H, 4.51; N, 6.27; Found, C, 69.70; H, 4.85; N, 6.00.

(3E,5E)-3,5-bis(4-fluorobenzylidene)-4-oxo-N-phenylpiperidine-1-carbothioamide (27)

The title compound was synthesized from (3E,5E)-3,5-bis(2-fluorobenzylidene)piperidin-4-one (**9**) and phenyl isothiocyanate in 86% yield as yellow solid. mp: 182–184 °C; IR (KBr) ν (cm^{-1}): 3419, 1644, 1385, 1215, 770; ^1H NMR (400 MHz, $\text{DMSO}-d_6$): δ 9.62 (s, 1H), 7.67–7.62 (m, 6H), 7.25–7.24 (m, 6H), 7.17–7.08 (m, 3H), 5.26 (s, 4H); ^{13}C (100 MHz, $\text{CDCl}_3+\text{DMSO}-d_6$): δ 191.5, 187.7, 169.0, 166.5, 145.8, 140.4, 138.1, 138.0, 136.9, 135.9, 133.2, 130.5, 129.8, 120.9, 120.7, 120.5, 54.2; ESI-MS: m/z 447 ($\text{M}+\text{H}^+$); HRMS (ESI): m/z calculated for $\text{C}_{26}\text{H}_{20}\text{F}_2\text{N}_2\text{O}_5\text{S} + \text{H}^+$ ($\text{M}+\text{H}^+$): 447.1343. Found: 447.1343. Elemental analysis (%) for $\text{C}_{26}\text{H}_{20}\text{F}_2\text{N}_2\text{O}_5\text{S}$: Calcd.: C, 69.94; H, 4.51; N, 6.27; Found, C, 69.86; H, 4.32; N, 6.47.

(3E,5E)-3,5-bis(2-methylbenzylidene)-4-oxo-N-phenylpiperidine-1-carbothioamide (28)

The title compound was synthesized from (3E,5E)-3,5-bis(2-methylbenzylidene)piperidin-4-one (**10**) and phenyl isothiocyanate in 87% yield as yellow solid. mp: 189–191 °C; IR (KBr) ν (cm^{-1}): 3401, 3019, 1618, 1403, 1215; ^1H NMR (400 MHz, CDCl_3): δ 8.02 (s, 2H), 7.30–7.23 (m, 4H), 7.22–7.17 (m, 4H), 7.12 (d, $J = 7.4$ Hz, 2H), 7.08–7.04 (m, 1H), 6.99 (s, 1H), 6.94 (d, $J = 7.4$ Hz, 2H), 4.94 (d, $J = 1.56$ Hz, 4H), 2.38 (s, 6H); ^{13}C (100 MHz, $\text{DMSO}-d_6$): δ 187.0, 183.3, 141.1, 138.2, 136.0, 133.9, 132.9, 130.7, 129.7, 129.4, 128.5, 126.3, 125.2, 124.9, 49.6, 20.1; ESI-MS: m/z 439 ($\text{M}+\text{H}^+$); HRMS (ESI): m/z calculated for $\text{C}_{28}\text{H}_{26}\text{N}_2\text{O}_5\text{S} + \text{H}^+$ ($\text{M}+\text{H}^+$): 439.1844. Found: 439.1840. Elemental analysis (%) for $\text{C}_{28}\text{H}_{26}\text{N}_2\text{O}_5\text{S}$: Calcd.: C, 76.68; H, 5.98; N, 6.39; Found, C, 76.44; H, 5.90; N, 6.19.

(3E,5E)-3,5-bis(4-methylbenzylidene)-4-oxo-N-phenylpiperidine-1-carbothioamide (29)

The title compound was synthesized from (3E,5E)-3,5-bis(4-methylbenzylidene)piperidin-4-one (**11**) and phenyl isothiocyanate in 80% yield as yellow solid. mp: 198–200 °C; IR (KBr) ν (cm^{-1}): 3410, 3022, 1640, 1524, 1217; ^1H NMR (400 MHz, $\text{CDCl}_3+\text{DMSO}-d_6$): δ 9.44 (s, 1H), 7.69 (s, 2H), 7.41–7.37 (m, 4H), 7.25–7.17 (m, 6H), 7.15–7.13 (m, 2H), 7.10–7.07 (m, 1H), 5.25 (s, 4H), 2.38 (s, 6H); ^{13}C (100 MHz, $\text{CDCl}_3+\text{DMSO}-d_6$): δ 191.5, 187.8, 145.8, 144.5, 141.7, 136.6, 136.0, 135.7, 134.3, 133.1, 130.3, 129.8, 54.4, 26.2; ESI-MS: m/z 439 ($\text{M}+\text{H}^+$); Elemental analysis (%) for $\text{C}_{28}\text{H}_{26}\text{N}_2\text{O}_5\text{S}$: Calcd.: C, 76.68; H, 5.98; N, 6.39; Found, C, 76.90; H, 5.69; N, 6.45.

(3E,5E)-3,5-bis(4-methoxybenzylidene)-4-oxo-N-phenylpiperidine-1-carbothioamide (30)

The title compound was synthesized from (3E,5E)-3,5-bis(2-fluorobenzylidene)piperidin-4-one (**12**) and phenyl isothiocyanate in 88% yield as yellow solid. mp: 168–170 °C; IR (KBr) ν (cm⁻¹): 3410, 1634, 1402, 1215, 1068; ¹H NMR (400 MHz, CDCl₃): δ 7.76 (s, 2H), 7.41 (s, 1H), 7.33 (d, *J* = 8.7 Hz, 4H), 7.21–7.17 (m, 2H), 7.06–7.02 (m, 3H), 6.93 (d, *J* = 8.8 Hz, 4H), 5.10 (d, *J* = 1.3 Hz, 4H), 3.86 (s, 6H); ¹³C (100 MHz, CDCl₃+DMSO-*d*₆): δ 191.6, 187.8, 165.4, 145.5, 141.8, 137.5, 134.2, 133.2, 132.0, 129.9, 119.0, 60.1, 54.5; ESI-MS: *m/z* 471 (M+H⁺); HRMS (ESI): *m/z* calculated for C₂₈H₂₆N₂O₃S + H⁺ (M+H⁺): 471.1742. Found: 471.1742. Elemental analysis (%) for C₂₈H₂₆N₂O₃S: Calcd.: C, 71.46; H, 5.57; N, 5.95; Found, C, 71.65; H, 5.74; N, 5.80.

(3E,5E)-3,5-bis(4-isopropylbenzylidene)-4-oxo-N-phenylpiperidine-1-carbothioamide (31)

The title compound was synthesized from (3E,5E)-3,5-bis(4-isopropylbenzylidene)piperidin-4-one (**13**) and phenyl isothiocyanate in 80% yield as yellow solid. mp: 178–180 °C; IR (KBr) ν (cm⁻¹): 3412, 3019, 1640, 1215; ¹H NMR (400 MHz, CDCl₃): δ 7.82 (s, 2H), 7.33–7.27 (m, 8H), 7.17–7.13 (m, 3H), 7.03–6.95 (m, 3H), 5.12 (d, *J* = 1.5 Hz, 4H), 3.01–2.91 (m, 2H), 1.29 (d, *J* = 6.9 Hz, 12H); ¹³C (100 MHz, CDCl₃): δ 186.5, 183.5, 151.0, 139.5, 138.3, 131.8, 130.7, 130.0, 128.9, 126.9, 125.2, 122.8, 50.4, 34.0, 23.7; ESI-MS: *m/z* 495 (M+H⁺); HRMS (ESI): *m/z* calculated for C₃₂H₃₄N₂O₃S + H⁺ (M+H⁺): 495.2470. Found: 495.2469. Elemental analysis (%) for C₃₂H₃₄N₂O₃S: Calcd.: C, 77.69; H, 6.93; N, 5.66; Found, C, 77.56; H, 6.77; N, 5.55.

N-((3E,5E)-3,5-bis(2-fluorobenzylidene)-4-oxopiperidine-1-carbonothioyl)benzamide (32)

The title compound was synthesized from (3E,5E)-3,5-bis(2-fluorobenzylidene)piperidin-4-one (**8**) and benzoyl isothiocyanate in 76% yield as yellow solid. mp: 155–157 °C; IR (KBr) ν (cm⁻¹): 3400, 3020, 1743, 1626, 1385, 1215, 758; ¹H NMR (400 MHz, CDCl₃+DMSO-*d*₆): δ 10.38 (s, 1H), 7.88 (s, 2H), 7.66–7.62 (m, 2H), 7.50–7.08 (m, 11H), 5.34–4.85 (m, 4H); ¹³C (100 MHz, CDCl₃+DMSO-*d*₆): δ 189.8, 186.2, 169.4, 166.5, 164.0, 137.5, 137.1, 137.1, 136.5, 135.5, 133.0, 133.0, 129.2, 126.9, 120.7, 120.5, 55.7; ESI-MS: *m/z* 475 (M+H⁺); HRMS (ESI): *m/z* calculated for C₂₇H₂₀F₂N₂O₂S + H⁺ (M+H⁺): 475.1292. Found: 475.1293. Elemental analysis (%) for C₂₇H₂₀F₂N₂O₂S: Calcd.: C, 68.34; H, 4.25; N, 5.90; Found, C, 68.01; H, 4.50; N, 6.10.

N-((3E,5E)-3,5-bis(4-fluorobenzylidene)-4-oxopiperidine-1-carbonothioyl)benzamide (33)

The title compound was synthesized from (3E,5E)-3,5-bis(4-fluorobenzylidene)piperidin-4-one (**9**) and benzoyl isothiocyanate in 79% yield as yellow solid. mp: 163–165 °C; IR (KBr) ν (cm⁻¹): 3400, 3019, 1744, 1620, 1385, 1215, 757; ¹H NMR (400 MHz, CDCl₃+DMSO-*d*₆): δ 10.41 (s, 1H), 7.79 (s, 2H), 7.69–7.62 (m, 2H), 7.52–6.95 (m, 11H), 5.45–4.91 (m, 4H); ¹³C (100 MHz, DMSO-*d*₆): δ 185.4, 181.4, 164.8, 164.3, 161.6, 137.0, 136.6, 133.3, 132.7, 132.6, 131.2, 128.5, 128.4, 116.1, 50.7; ESI-MS: *m/z* 475 (M+H⁺); HRMS (ESI): *m/z* calculated for C₂₇H₂₀F₂N₂O₂S + H⁺ (M+H⁺): 475.1292. Found: 475.1287. Elemental analysis (%) for C₂₇H₂₀F₂N₂O₂S: Calcd.: C, 68.34; H, 4.25; N, 5.90; Found, C, 68.40; H, 4.63; N, 6.12.

N-((3E,5E)-3,5-bis(2-methylbenzylidene)-4-oxopiperidine-1-carbonothioyl)benzamide (34)

The title compound was synthesized from (3E,5E)-3,5-bis(2-methylbenzylidene)piperidin-4-one (**10**) and benzoyl isothiocyanate in 76% yield as yellow solid. mp: 159–161 °C; IR (KBr) ν (cm⁻¹): 3408, 3019, 1741, 1621, 1403, 1215; ¹H NMR (400 MHz, CDCl₃): δ 8.24 (s, 1H), 8.05 (s, 2H), 7.55–7.53 (m, 3H), 7.42–7.38 (m, 2H), 7.28–7.05 (m, 8H), 5.16–4.87 (m, 4H), 2.39 (s, 6H); ¹³C (100 MHz, DMSO-*d*₆): δ 185.6, 181.0, 164.6, 137.2, 132.6, 131.9, 130.6, 129.2, 128.5, 128.2, 126.3, 125.7, 51.2, 50.5, 20.0; ESI-MS: *m/z* 467 (M+H⁺); HRMS (ESI): *m/z* calculated for C₂₉H₂₆N₂O₂S + H⁺ (M+H⁺): 467.1793. Found: 467.1793. Elemental analysis (%) for C₂₉H₂₆N₂O₂S: Calcd.: C, 74.65; H, 5.62; N, 6.00; Found, C, 74.44; H, 5.34; N, 6.18.

N-((3E,5E)-3,5-bis(4-methylbenzylidene)-4-oxopiperidine-1-carbonothioyl)benzamide (35)

The title compound was synthesized from (3E,5E)-3,5-bis(4-methylbenzylidene)piperidin-4-one (**11**) and benzoyl isothiocyanate in 70% yield as yellow solid. mp: 205–207 °C; IR (KBr) ν (cm⁻¹): 3410, 3025, 1732, 1644, 1216; ¹H NMR (400 MHz, CDCl₃+DMSO-*d*₆): δ 10.56 (s, 1H), 7.77 (s, 2H), 7.63 (d, *J* = 7.2 Hz, 2H), 7.52–7.16 (m, 11H), 5.52–4.93 (m, 4H), 2.38–2.26 (m, 6H); ¹³C (100 MHz, DMSO-*d*₆): δ 190.2, 186.0, 169.6, 145.1, 142.7, 137.5, 137.3, 136.5, 135.7, 135.4, 134.4, 133.3, 133.1, 56.0, 26.1; ESI-MS: *m/z* 467 (M+H⁺); HRMS (ESI): *m/z* calculated for C₂₉H₂₆N₂O₂S + H⁺ (M+H⁺): 467.1793. Found: 467.1786. Elemental analysis (%) for C₂₉H₂₆N₂O₂S: Calcd.: C, 74.65; H, 5.62; N, 6.00; Found, C, 74.52; H, 5.37; N, 6.34.

N-((3E,5E)-3,5-bis(4-methoxybenzylidene)-4-oxopiperidine-1-carbonothioyl)benzamide (36)

The title compound was synthesized from (3E,5E)-3,5-bis(4-fluorobenzylidene)piperidin-4-one (**12**) and benzoyl isothiocyanate in 82% yield as yellow solid. mp: 178–180 °C; IR (KBr) ν (cm⁻¹): 3401, 3019, 1743, 1618, 1385, 1215, 1068; ¹H NMR (400 MHz, CDCl₃+DMSO-*d*₆): δ 7.86 (s, 2H), 7.78 (s, 1H), 7.65–7.63 (m, 2H), 7.59–7.55 (m, 1H), 7.44–7.36 (m, 6H), 6.97–6.88 (m, 4H), 5.43–5.07 (m, 4H), 3.87–3.81 (m, 6H); ¹³C (100 MHz, DMSO-*d*₆): δ 185.2, 181.2, 164.8, 160.8, 137.5, 134.3, 133.6, 132.8, 132.6, 129.4, 128.5, 128.4, 127.9, 127.1, 114.7, 55.7, 51.3; ESI-MS: *m/z* 499 (M+H⁺); HRMS (ESI): *m/z* calculated for C₂₉H₂₆N₂O₄S + H⁺ (M+H⁺): 499.1692. Found: 499.1674. Elemental analysis (%) for C₂₉H₂₆N₂O₄S: Calcd.: C, 69.86; H, 5.26; N, 5.62; Found, C, 69.70; H, 5.01; N, 5.88.

N-((3E,5E)-3,5-bis(4-isopropylbenzylidene)-4-oxopiperidine-1-carbonothioyl)benzamide (37)

The title compound was synthesized from (3E,5E)-3,5-bis(4-isopropylbenzylidene)piperidin-4-one (**13**) and benzoyl isothiocyanate in 71% yield as yellow solid. mp: 175–177 °C; IR (KBr) ν (cm⁻¹): 3411, 3030, 1735, 1620, 1216; ¹H NMR (400 MHz, DMSO-*d*₆): δ 10.79 (s, 1H), 7.78–7.71 (m, 2H), 7.58–7.50 (m, 5H), 7.42–7.28 (m, 6H), 7.14–7.13 (m, 2H), 5.59–4.98 (m, 4H), 2.97–2.77 (m, 2H), 1.24–1.06 (m, 12H); ESI-MS: *m/z* 523 (M+H⁺); HRMS (ESI): *m/z* calculated for C₃₃H₃₄N₂O₂S + H⁺ (M+H⁺): 523.2419. Found: 523.2408. Elemental analysis (%) for C₃₃H₃₄N₂O₂S: Calcd.: C, 75.83; H, 6.56; N, 5.36; Found, C, 75.99; H, 6.70; N, 5.04.

(3E,5E)-N-butyl-3,5-bis(2-fluorobenzylidene)-4-oxopiperidine-1-carbothioamide (38)

The title compound was synthesized from (3E,5E)-3,5-bis(2-fluorobenzylidene)piperidin-4-one (**8**) and butyl isothiocyanate in 71% yield as yellow solid. mp: 163–165 °C; IR (KBr) ν (cm⁻¹): 3418, 3120, 1621, 1384, 1215, 757; ¹H NMR (400 MHz, CDCl₃): δ 7.89 (s, 2H), 7.47–7.40 (m, 4H), 7.28–7.24 (m, 2H), 7.21–7.16 (m, 2H), 5.13 (s, 1H), 4.97 (s, 4H), 3.48–3.43 (m, 2H), 1.34–1.27 (m, 2H), 1.14–1.07 (m, 2H), 0.82 (t, J = 7.3 Hz, 3H); ¹³C (100 MHz, CDCl₃): δ 186.2, 182.2, 161.9, 159.4, 133.2, 131.7, 131.6, 130.9, 130.9, 130.8, 124.5, 124.4, 122.2, 122.1, 116.2, 116.0, 48.8, 46.1, 30.7, 19.8, 13.7; ESI-MS: m/z 427 (M+H⁺); HRMS (ESI): m/z calculated for C₂₄H₂₄F₂N₂OS + H⁺ (M+H⁺): 427.1656. Found: 427.1654. Elemental analysis (%) for C₂₄H₂₄F₂N₂OS: Calcd.: C, 67.58; H, 5.67; N, 6.57; Found, C, 67.30; H, 5.98; N, 6.47.

(3E,5E)-N-butyl-3,5-bis(4-fluorobenzylidene)-4-oxopiperidine-1-carbothioamide (39)

The title compound was synthesized from (3E,5E)-3,5-bis(4-fluorobenzylidene)piperidin-4-one (**9**) and butyl isothiocyanate in 81% yield as yellow solid. mp: 176–178 °C; IR (KBr) ν (cm⁻¹): 3408, 3090, 1640, 1385, 1215, 768; ¹H NMR (400 MHz, CDCl₃): δ 7.81 (s, 2H), 7.47 (d/d, J_1 = 5.3 Hz, J_2 = 8.7 Hz, 4H), 7.21–7.17 (m, 4H), 5.07 (d, J = 1.12 Hz, 4H), 5.03 (s, 1H), 3.47–3.42 (m, 2H), 1.30–1.23 (m, 2H), 1.14–1.04 (m, 2H), 0.81 (t, J = 7.2 Hz, 3H); ¹³C (100 MHz, CDCl₃+DMSO-*d*₆): δ 191.9, 187.1, 168.7, 166.7, 140.4, 140.3, 137.7, 136.7, 135.7, 120.7, 120.6, 53.3, 50.7, 35.8, 24.7, 18.7; ESI-MS: m/z 427 (M+H⁺); HRMS (ESI): m/z calculated for C₂₄H₂₄F₂N₂OS + H⁺ (M+H⁺): 427.1656. Found: 427.1658. Elemental analysis (%) for C₂₄H₂₄F₂N₂OS: Calcd.: C, 67.58; H, 5.67; N, 6.57; Found, C, 67.90; H, 5.81; N, 6.30.

(3E,5E)-N-butyl-3,5-bis(2-methylbenzylidene)-4-oxopiperidine-1-carbothioamide (40)

The title compound was synthesized from (3E,5E)-3,5-bis(2-methylbenzylidene)piperidin-4-one (**10**) and butyl isothiocyanate in 71% yield as yellow solid. mp: 152–154 °C; IR (KBr) ν (cm⁻¹): 3410, 3019, 1620, 1215; ¹H NMR (400 MHz, CDCl₃): δ 8.00 (s, 2H), 7.37–7.24 (m, 8H), 4.92 (d, J = 1.2 Hz, 4H), 4.86 (s, 1H), 3.42 (q, J_1 = 7.0 Hz, J_2 = 11.8, 2H), 2.39 (s, 6H), 1.25–1.18 (m, 2H), 1.10–1.01 (m, 2H), 0.80 (t, J = 7.2 Hz, 3H); ¹³C (100 MHz, CDCl₃): δ 187.2, 181.8, 138.2, 137.3, 133.2, 131.9, 130.7, 129.6, 128.9, 126.0, 48.4, 46.0, 30.7, 20.1, 19.8, 13.7; ESI-MS: m/z 419 (M+H⁺); HRMS (ESI): m/z calculated for C₂₆H₃₀N₂OS + H⁺ (M+H⁺): 419.2157. Found: 419.2154. Elemental analysis (%) for C₂₆H₃₀N₂OS: Calcd.: C, 74.60; H, 7.22; N, 6.69; Found, C, 74.50; H, 7.52; N, 6.99.

(3E,5E)-N-butyl-3,5-bis(4-methylbenzylidene)-4-oxopiperidine-1-carbothioamide (41)

The title compound was synthesized from (3E,5E)-3,5-bis(4-methylbenzylidene)piperidin-4-one (**11**) and butyl isothiocyanate in 75% yield as yellow solid. mp: 194–196 °C; IR (KBr) ν (cm⁻¹): 3411, 3019, 1644, 1215; ¹H NMR (400 MHz, CDCl₃): δ 7.83 (s, 2H), 7.37 (d, J = 8.1 Hz, 4H), 7.29 (d, J = 8.1 Hz, 4H), 5.09 (d, J = 1.1 Hz, 4H), 4.93 (s, 1H), 3.41 (q, J_1 = 7.0 Hz, J_2 = 11.7 Hz, 2H), 2.43 (s, 6H), 1.21–1.14 (m, 2H), 1.09–0.99 (m, 2H), 0.78 (t, J = 7.2 Hz, 3H); ¹³C (100 MHz, CDCl₃+DMSO-*d*₆): δ 191.9, 187.1, 144.4, 141.3, 141.2, 136.7, 136.5, 135.7, 134.4, 53.6,

50.6, 35.8, 26.2, 24.7, 18.8; ESI-MS: m/z 419 (M+H⁺); HRMS (ESI): m/z calculated for C₂₆H₃₀N₂OS + H⁺ (M+H⁺): 419.2157. Found: 419.2158. Elemental analysis (%) for C₂₆H₃₀N₂OS: Calcd.: C, 74.60; H, 7.22; N, 6.69; Found, C, 74.33; H, 7.42; N, 6.96.

(3E,5E)-N-butyl-3,5-bis(4-methoxybenzylidene)-4-oxopiperidine-1-carbothioamide (42)

The title compound was synthesized from (3E,5E)-3,5-bis(4-fluorobenzylidene)piperidin-4-one (**12**) and butyl isothiocyanate in 80% yield as yellow solid. mp: 164–166 °C; IR (KBr) ν (cm⁻¹): 3410, 3020, 1635, 1390, 1215, 1030; ¹H NMR (400 MHz, CDCl₃): δ 7.80 (s, 2H), 7.44 (d, J = 8.8 Hz, 4H), 7.01 (d, J = 8.8 Hz, 4H), 5.09 (d, J = 1.0 Hz, 4H), 4.99 (s, 1H), 3.88 (s, 6H), 3.45–3.41 (m, 2H), 1.25–1.18 (m, 2H), 1.11–1.02 (m, 2H), 0.79 (t, J = 7.2 Hz, 3H); ¹³C (100 MHz, CDCl₃): δ 186.9, 182.2, 160.8, 137.5, 132.4, 129.7, 126.9, 114.4, 55.4, 48.8, 46.1, 30.7, 19.8, 13.7; ESI-MS: m/z 451 (M+H⁺); HRMS (ESI): m/z calculated for C₂₆H₃₀N₂O₃S + H⁺ (M+H⁺): 451.2055. Found: 451.2055. Elemental analysis (%) for C₂₆H₃₀N₂O₃S: Calcd.: C, 69.30; H, 6.71; N, 6.22; Found, C, 69.41; H, 6.99; N, 6.00.

(3E,5E)-N-butyl-3,5-bis(4-isopropylbenzylidene)-4-oxopiperidine-1-carbothioamide (43)

The title compound was synthesized from (3E,5E)-3,5-bis(4-isopropylbenzylidene)piperidin-4-one (**13**) and butyl isothiocyanate in 77% yield as yellow solid. mp: 116–118 °C; IR (KBr) ν (cm⁻¹): 3411, 3019, 1640, 1218; ¹H NMR (400 MHz, CDCl₃): δ 7.83 (s, 2H), 7.41 (d, J = 8.2 Hz, 4H), 7.35 (d, J = 8.2 Hz, 4H), 5.10 (d, J = 1.1 Hz, 4H), 4.92 (s, 1H), 3.43–3.38 (m, 2H), 3.03–2.93 (m, 2H), 1.30 (d, J = 6.9 Hz, 12H), 1.20–1.11 (m, 2H), 1.09–1.02 (m, 2H), 0.78 (t, J = 7.2 Hz, 3H); ¹³C (100 MHz, CDCl₃): δ 187.2, 182.1, 151.1, 137.9, 131.8, 130.9, 130.6, 127.1, 48.8, 45.9, 34.0, 30.6, 23.7, 19.7, 13.7; ESI-MS: m/z 475 (M+H⁺); HRMS (ESI): m/z calculated for C₃₀H₃₈N₂OS + H⁺ (M+H⁺): 475.2783. Found: 475.2782. Elemental analysis (%) for C₃₀H₃₈N₂OS: Calcd.: C, 75.90; H, 8.07; N, 5.90; Found, C, 76.11; H, 8.31; N, 5.63.

(3E,5E)-3,5-bis(2-fluorobenzylidene)-1-(4-phenylthiazol-2-yl)piperidin-4-one (44)

The title compound was synthesized from (3E,5E)-3,5-bis(2-fluorobenzylidene)piperidin-4-one (**8**) and phenacyl thiocyanate in 73% yield as yellow solid. mp: 110–112 °C; IR (KBr) ν (cm⁻¹): 3109, 1620, 1454, 1218, 761; ¹H NMR (400 MHz, CDCl₃): δ 7.97 (s, 2H), 7.60 (d, J = 6.8, 2H), 7.48–7.44 (m, 4H), 7.32–7.26 (m, 4H), 7.25–7.19 (m, 3H), 6.73 (s, 1H), 4.79 (s, 4H); ¹³C (100 MHz, DMSO-*d*₆): δ 186.2, 169.2, 162.0, 159.6, 150.9, 134.5, 134.5, 132.4, 132.3, 131.6, 130.6, 130.6, 128.8, 128.0, 125.9, 125.1, 125.1, 122.6, 122.5, 116.4, 116.2, 104.8, 50.1; ESI-MS: m/z 471 (M+H⁺); Elemental analysis (%) for C₂₈H₂₀F₂N₂OS: Calcd.: C, 71.47; H, 4.28; N, 5.95; Found, C, 71.72; H, 4.49; N, 6.28.

(3E,5E)-3,5-bis(4-fluorobenzylidene)-1-(4-phenylthiazol-2-yl)piperidin-4-one (45)

The title compound was synthesized from (3E,5E)-3,5-bis(4-fluorobenzylidene)piperidin-4-one (**9**) and phenacyl thiocyanate in 75% yield as yellow solid. mp: 191–193 °C; IR (KBr) ν (cm⁻¹): 3021, 1626, 1406, 1216, 762; ¹H NMR (400 MHz, CDCl₃): δ 7.88 (s, 2H), 7.63 (d, J = 6.9, 2H), 7.50 (d/d, J_1 = 5.4 Hz,

$J_2 = 8.6$, 4H), 7.34–7.27 (m, 3H), 7.23–7.19 (m, 4H), 6.75 (s, 1H), 4.89 (d, $J = 1.5$, 4H); ^{13}C (100 MHz, $\text{CDCl}_3 + \text{DMSO}-d_6$): δ 191.1, 173.9, 169.1, 166.6, 156.3, 142.0, 139.2, 137.2, 137.2, 136.2, 135.7, 133.1, 132.4, 130.5, 120.8, 120.6, 107.7, 54.5; ESI-MS: m/z 471 ($\text{M} + \text{H}^+$); HRMS (ESI): m/z calculated for $\text{C}_{28}\text{H}_{20}\text{F}_2\text{N}_2\text{O}_5\text{S} + \text{H}^+$ ($\text{M} + \text{H}^+$): 471.1343. Found: 471.1340. Elemental analysis (%) for $\text{C}_{28}\text{H}_{20}\text{F}_2\text{N}_2\text{O}_5\text{S}$: Calcd.: C, 71.47; H, 4.28; N, 5.95; Found, C, 71.19; H, 4.40; N, 5.79.

(3E,5E)-3,5-bis(2-methylbenzylidene)-1-(4-phenylthiazol-2-yl)piperidin-4-one (46)

The title compound was synthesized from (3E,5E)-3,5-bis(2-methylbenzylidene)piperidin-4-one (**10**) and phenacyl thiocyanate in 72% yield as yellow solid. mp: 105–107 °C; IR (KBr) ν (cm^{-1}): 3019, 1639, 1402, 1385, 1215; ^1H NMR (400 MHz, CDCl_3): δ 8.07 (s, 2H), 7.61 (d/d, $J_1 = 1.52$ Hz, $J_2 = 8.40$ Hz, 2H), 7.37–7.26 (m, 11H), 6.72 (s, 1H), 4.75 (d, $J = 1.64$ Hz, 4H), 2.35 (s, 6H); ^{13}C (100 MHz, CDCl_3): δ 187.2, 169.0, 151.8, 138.3, 138.2, 134.6, 134.0, 132.0, 130.4, 129.3, 129.0, 128.3, 127.6, 125.9, 125.7, 102.6, 50.0, 20.2; ESI-MS: m/z 463 ($\text{M} + \text{H}^+$); HRMS (ESI): m/z calculated for $\text{C}_{30}\text{H}_{26}\text{N}_2\text{O}_5\text{S} + \text{H}^+$ ($\text{M} + \text{H}^+$): 463.1844. Found: 463.1842. Elemental analysis (%) for $\text{C}_{30}\text{H}_{26}\text{N}_2\text{O}_5\text{S}$: Calcd.: C, 77.89; H, 5.66; N, 6.06; Found, C, 77.60; H, 5.74; N, 6.38.

(3E,5E)-3,5-bis(4-methylbenzylidene)-1-(4-phenylthiazol-2-yl)piperidin-4-one (47)

The title compound was synthesized from (3E,5E)-3,5-bis(4-methylbenzylidene)piperidin-4-one (**11**) and phenacyl thiocyanate in 74% yield as yellow solid. mp: 166–168 °C; IR (KBr) ν (cm^{-1}): 3019, 1644, 1403, 1220; ^1H NMR (400 MHz, CDCl_3): δ 7.91 (s, 2H), 7.66 (d, $J = 6.9$ Hz, 2H), 7.42 (d, $J = 8.0$ Hz, 4H), 7.33–7.26 (m, 7H), 6.74 (s, 1H), 4.93 (d, $J = 1.4$ Hz, 4H), 2.46 (s, 6H); ^{13}C (100 MHz, CDCl_3): δ 186.8, 169.4, 151.9, 139.8, 138.4, 134.7, 132.1, 130.8, 130.6, 129.5, 128.4, 127.6, 126.0, 102.5, 50.0, 21.5; ESI-MS: m/z 453 ($\text{M} + \text{H}^+$); HRMS (ESI): m/z calculated for $\text{C}_{30}\text{H}_{26}\text{N}_2\text{O}_5\text{S} + \text{H}^+$ ($\text{M} + \text{H}^+$): 463.1844. Found: 463.1844. Elemental analysis (%) for $\text{C}_{30}\text{H}_{26}\text{N}_2\text{O}_5\text{S}$: Calcd.: C, 77.89; H, 5.66; N, 6.06; Found, C, 77.99; H, 5.80; N, 6.35.

(3E,5E)-3,5-bis(4-methoxybenzylidene)-1-(4-phenylthiazol-2-yl)piperidin-4-one (48)

The title compound was synthesized from (3E,5E)-3,5-bis(4-methoxybenzylidene)piperidin-4-one (**12**) and phenacyl thiocyanate in 70% yield as yellow solid. mp: 197–199 °C; IR (KBr) ν (cm^{-1}): 3021, 1644, 1385, 1215, 1068; ^1H NMR (400 MHz, CDCl_3): δ 7.88 (s, 2H), 7.68 (d, $J = 7.0$, 2H), 7.49 (d, $J = 8.7$ Hz, 4H), 7.38–7.23 (m, 3H), 7.04 (d, $J = 8.8$ Hz, 4H), 6.75 (s, 1H), 4.93 (d, $J = 1.5$, 4H), 3.91 (s, 6H); ^{13}C (100 MHz, $\text{DMSO}-d_6$): δ 186.3, 169.7, 161.0, 151.0, 137.7, 134.6, 133.0, 132.8, 130.5, 128.8, 128.0, 127.5, 126.0, 114.8, 104.4, 55.8, 50.1; ESI-MS: m/z 495 ($\text{M} + \text{H}^+$); HRMS (ESI): m/z calculated for $\text{C}_{30}\text{H}_{26}\text{N}_2\text{O}_5\text{S} + \text{H}^+$ ($\text{M} + \text{H}^+$): 495.1742. Found: 495.1741. Elemental analysis (%) for $\text{C}_{30}\text{H}_{26}\text{N}_2\text{O}_5\text{S}$: Calcd.: C, 72.85; H, 5.30; N, 5.66; Found, C, 72.99; H, 5.25; N, 5.35.

(3E,5E)-3,5-bis(4-isopropylbenzylidene)-1-(4-phenylthiazol-2-yl)piperidin-4-one (49)

The title compound was synthesized from (3E,5E)-3,5-bis(4-isopropylbenzylidene)piperidin-4-one (**13**) and phenacyl thiocyanate in 79% yield as yellow solid. mp: 205–207 °C; IR

(KBr) ν (cm^{-1}): 3409, 3019, 1639, 1385, 1216; ^1H NMR (400 MHz, CDCl_3): δ 7.91 (s, 2H), 7.68 (d, $J = 6.9$ Hz, 2H), 7.47 (d, $J = 8.2$ Hz, 4H), 7.38 (d, $J = 8.2$ Hz, 4H), 7.33–7.27 (m, 3H), 6.75 (s, 1H), 4.94 (d, $J = 1.6$ Hz, 4H), 3.07–2.94 (m, 2H), 1.34 (d, $J = 6.9$ Hz, 12H); ^{13}C (100 MHz, $\text{CDCl}_3 + \text{DMSO}-d_6$): δ 191.3, 174.1, 156.3, 155.4, 143.0, 139.3, 137.1, 135.6, 135.4, 133.1, 132.3, 131.6, 130.6, 107.4, 54.7, 38.7, 28.5; ESI-MS: m/z 519 ($\text{M} + \text{H}^+$); HRMS (ESI): m/z calculated for $\text{C}_{34}\text{H}_{34}\text{N}_2\text{O}_5\text{S} + \text{H}^+$ ($\text{M} + \text{H}^+$): 519.2470. Found: 519.2467. Elemental analysis (%) for $\text{C}_{34}\text{H}_{34}\text{N}_2\text{O}_5\text{S}$: Calcd.: C, 78.73; H, 6.61; N, 5.40; Found, C, 78.58; H, 6.79; N, 5.71.

Biology

Molecular modelling and docking studies

MolDock is a docking module of Molegro Virtual Docker (MVD) software [22]. It is based on a new hybrid search algorithm, called guided differential evolution (DE). The guided DE algorithm combines the DE optimization techniques with a cavity prediction algorithm. DE was introduced by Storn and Price in 1995 and has previously been successfully applied to molecular docking [23]. The use of predicted cavities during the search process allows for a fast and accurate identification of potential binding modes (poses). The docking scoring function of MolDock is based on a piecewise linear potential (PLP) introduced by Gehlhaar *et al* [24]. In MolDock, the docking scoring function is extended with a new term, taking hydrogen bond directionality into account. Moreover, a re-ranking procedure was applied to the highest ranked poses to further increase docking accuracy. Initially, the protein was considered without ligand and water molecules. The backbone was fixed, the CharmM force field and minimization using steep descent algorithm was applied for selected protein and all the compounds were prepared using the CharmM force field and minimized up to a gradient of 0.01 kcal/(mol Å) with the help of Discovery Studio 2.5 software (Telesis Court, San Diego, CA) as reported previously [25]. Template docking is based on extracting the chemical properties like the pharmacophore elements of a ligand bound in the active site. This information is utilized in the docking of the structurally similar analogs. The PDB ID 1X9N was used as the template with the default settings for docking studies, including a grid resolution of 0.30, for grid generation and a 15 Å radius from the template as the binding site as reported previously [26]. MolDock SE was used as a search algorithm and the number of runs was set to 10. A population size of 50 and a maximum iteration of 1500 were used for parameter settings. The maximum number of poses generated was 10. Since Molegro Virtual Docker works by an evolutionary algorithm, consecutive docking runs do not give exactly the same pose and interactions as reported previously by our group [27–31]. To address this inherent randomness, three consecutive runs were done and the top three poses were used to visualize the interactions of all inhibitors.

Common feature pharmacophore generation

ARTICLE

Journal Name

The set of ten diverse compounds reported as hLigI inhibitors were used as a training set (Figure 1). Pharmacophore generation was performed on a Windows-based operating system having an Intel Pentium dual core 2.8 GHz processor using the Hiphop algorithm of CATALYST implemented in the Discovery Studio 2.0 software package (DS 2.0). All compounds used in the study were built using ISIS Draw 2.5 and imported to DS 2.0 Windows. These compounds were optimized using the CHARMM force field [25]. The conformation of these compounds were generated in the diverse conformation generation protocol of the DS with the parameters of 255 conformations with the energy cut off range of 20 kcal/mol above the global minimum. In the DS, the principal value of 2 and maximum omit feature were assigned to 0 for all compounds to assign them as most active compounds. Minimum inter-feature distance was set to 2 Å from the default value of 2.97 Å in order to consider the functional groups that are present in the training set compounds as closely as 2 Å. This has been done to include the closely related functional groups present in the training set compounds (C=O and –OH) in carboxylic acid which are present in most of the training set compounds involved in the hLigI inhibition. Feature mapping protocol was used to identify the common features present in the training set compounds. As predicted, HBAL (min. 1 - max. 5), RA (min. 1- max. 5), and HBD (min. 1 - max. 5) were selected during the pharmacophore generation (Figure 3).

Purification of HLigI

The clone for HLigI (pRSFDuet-LigI) was a kind gift from Prof. Alan Tomkinson (University of New Mexico, Albuquerque, USA). This clone was transformed into BL21DE3RP cells (Agilent Technologies) and the protein was expressed at 16 °C for 18 hr after induction with 1 mM IPTG. The protein was purified following a reported protocol [32] with slight modifications. Briefly, cells were lysed in a buffer containing 50 mM Tris-Cl (pH 7.5), 50 mM NaCl, 10% glycerol and protease inhibitors PMSF, benzamidine etc. The cells were lysed by sonication (15 times with 10 sec start and 10 sec stop pulses) with a probe sonicator. After sonication, anionic detergent NP-40 was added to a final concentration of 1% and mixed by inverting and the lysate was centrifuged at 20,000 g for 30 min. After centrifugation, the clear lysate was filtered through a 0.45 micron filter to remove all insoluble impurities. The lysate was then loaded onto a 10 ml phosphocellulose column packed manually. This allowed the over-expressed ligase protein to bind with the phosphocellulose. The column were then washed with 5X volume of buffer containing 50 mM Tris-Cl (pH 7.5), 50 mM NaCl, 10% glycerol and protease inhibitors to remove all unbound proteins. After this, incremental concentrations of NaCl (50 mM, 100 mM and 200 mM) in the same buffer were used to remove non-specifically bound impurities and finally the ligase I protein was eluted at 300mM NaCl concentration. The eluted fraction of protein was dialysed against buffer containing 50 mM Tris-Cl (pH 7.5), 50 mM NaCl, 10% glycerol and the protease inhibitor PMSF and

loaded onto a 5ml pre-packed heparin column. This allowed the ligase protein to bind to heparin. The heparin column was then washed following the same procedure for phosphocellulose column. Finally, the ligase I protein was eluted from the heparin column at 300 mM NaCl concentration. For additional purity, the protein was finally purified through a gel-filtration column through the AKTA protein purification system (GE Life sciences). The purified protein was run on a SDS PAGE to check for purity, estimated by the Bradford method and then used for ligation assays.

In vitro DNA ligation assay

DNA ligation assay was performed as described previously [3e]. For the preparation of DNA substrate three different single strand DNA oligos were used, 52-mer (5'-GTACGTCGATCGATTGGTAGATCAGTGTCTATGTATGTCAGTGAG ATAGTAC-3'), 25-mer (5'-CTGATCTACCAATCGATCGACGTAC-3') and 27-mer (5'-/5Cy3/GTACTATCTCACTGACATACATAGACA-3'). First we have phosphorylated the 25-mer oligo. We have incubated 100 pmol of 25-mer with 30 units of T4 polynucleotide kinase and 2 µM of ATP in 1X PNK buffer for 1 hr at 37 °C. Then these oligos were annealed to form a double-stranded nicked DNA substrate for the ligase enzymes. For the easy detection of DNA oligos, 5' end of 27-mer oligo was labelled with a fluorescent dye Cyanin3 (Cy3). Ligation assay was performed in 20 µL of reaction mixture that contained 1 pmol of labelled DNA substrate and 0.2 pmol of purified hLigI in a ligation buffer containing Tris-Cl (50 mM, pH 7.5), MgCl₂ (10 mM), BSA (0.25 mg/ml), NaCl (100 mM) and ATP (500 µM). The reaction mixtures were incubated in the absence or presence of compounds at 37 °C for 30 min. To stop the ligation reactions, stop buffer (90% formamide and 10% of 50 mM EDTA) was used. The ligated and un-ligated products were separated by running the reaction mixtures in denaturing gel containing 7 M urea and 12% acrylamide. GE Image quant LAS 4010 was used for taking the gel picture and for estimating the density of ligated and un-ligated products.

Electrophoretic mobility shift assay (EMSA)

Electrophoretic mobility shift assay was performed as described in our previous work [3e]. Briefly, double stranded non-ligatable nicked DNA substrate was used for the study of interaction between compound and protein by electrophoretic mobility shift assay (EMSA). Three different oligos were used to make the substrate. One was a 5'-FAM labelled 27-mer oligo with a dideoxy modified 3' end (5'-/56-FAM/GTAC TATCTCACTGACATACATAGAC/3ddc/-3'). Other two oligos were 25-mer (25-mer was phosphorylated as described in previous section, 5'-CTGATCTACCAATCGATCGACGTAC-3') and 52-mer (5'-GTACGTCGATCGATTGGTAGATCAGGGTCTATGTATGTCAGTG AGATAGTAC-3') which were annealed to generate a non-ligatable nicked DNA substrate for ligase I protein. In the EMSA reaction 10 pmole of hLigI was incubated with 2 pmole of DNA in the presence of different concentrations (0, 100, 200, 500, 700 µM) of compound **23** in a ligation buffer containing Tris-Cl

(50 mM, pH 7.5), MgCl_2 (10 mM), BSA (0.25 mg/ml), NaCl (100 mM) and ATP (500 μM). The reaction mixtures were incubated on ice for 2 h. After the incubation 10 μL of native gel buffer Tris-Cl (50 mM, pH 7.5), 20% glycerol, 0.05% bromophenol blue) was added in each reaction, then samples were separated on a 6.5% native PAGE and bands were detected by GE Image quant LAS4010.

Gel retardation assay

DNA intercalation assay was performed for the study of interaction between compound **23** and DNA. As described previously [3e] with some modifications, here we have used positive controls for all kinds of DNA binders which are doxorubicin (DNA intercalator), DAPI (DNA minor groove binder) and methyl green (DNA major groove binder). We incubated 100 ng of linearized pUC18 plasmid with increasing concentrations (500, 700 μM) of compound **23** for 30 min at 37°C before running the samples in an agarose gel. Doxorubicin was used at 100 μM while ampicillin (negative control), DAPI and methyl green were used at 700 μM concentrations each. After the incubation, reaction products were resolved on a 1% agarose gel run at 5.3 V/cm. DNA in the gel was visualized by ethidium bromide staining.

DNase I protection assay

To check the direct interaction of compound with DNA, we have applied the concept of DNase I footprinting [33]. For this experiment we incubated 100 ng of plasmid DNA (pUC18) with 100 μM concentration of doxorubicin, 700 μM concentration of DAPI, methyl green compound **23** and ampicillin for 30 min at 37°C in an incubation buffer similar to ligation buffer. After incubation, the DNA was cleaved by adding 0.0025U of DNase1 in each reaction mixture for 5 min at 37°C and the reactions were stopped by adding stop buffer which contained 7M Urea, 20 mM Tris-Cl (pH. 7.5), 50 mM EDTA, 20% glycerol and Bromophenol blue. The samples were resolved on 1% agarose gel and visualized under UV transilluminator and image taken with GE Image quant LAS 4010.

Cell culture and viability assays

The human hepatic cancer (HepG2), breast cancer (MDA-MB-231) and mouse fibroblast (3T3) cell lines (ATCC, Manassas, VA) were grown in DMEM. Mouse breast cancer cell line 4T1 (ATCC, Manassas, VA) and human colon cancer cell line DLD-1 (ECACC, Salisbury, UK) were cultured in RPMI 1640. HCT116 (ECACC, Salisbury, UK) was cultured in McCoy's 5A media. Human cervical cancer cell line (HeLa) and human colon cancer cell line (HT-29) was obtained from NCCS (National Centre for Cell Science), Pune, India, and they were cultured in RPMI 1640 and McCoy's 5A media respectively. Media were supplemented with 10% (v/v) fetal bovine serum (FBS) and 1% antibiotic-antimycotic solution. Compounds to be screened were obtained as powder and dissolved in DMSO (Sigma St. Louis, MO) as 10mM stocks. MTT assay was performed as

described by ATCC, Manassas, VA. For MTT assay, cells were seeded in 96 well plates and incubated overnight. After incubation, cells were treated with five different concentrations of compounds (50, 25, 12.5, 6.3 and 3.1 μM) in triplicates for 48 h. Subsequently, 10 μL of MTT (5 mg/mL) was added to each well and incubated for 3 h. The MTT formazan formed by viable cells was dissolved in 100 μL of DMSO and shaken for 10 min or until it dissolved at room temperature. Absorbance was measured at 590 nm on a plate reader (Epoch Microplate Reader, Biotek, USA). The percentage inhibition in cell growth was calculated as per the formula $[(100 - (\text{Absorbance of inhibitor treated cells} / \text{Absorbance of control cells})) \times 100]$ and reported as average of three independent biological experiments.

Annexin V-FITC flow cytometry analysis

Compound **23** induced apoptosis in DLD1 cells was measured by using a commercially available Annexin V-FITC apoptosis detection kit (BD Biosciences, San Diego, CA). Briefly, cells were seeded in 6 well plates and treated with different concentrations (4.5 and 9 μM) of compound **23** for 48 hr. The cells were then harvested, washed with cold PBS and stained with Annexin V-FITC and propidium iodide (PI) in binding buffer according to manufacturer's instructions. The stained cells were analyzed by fluorescence-activated cell sorting using a FACS-Calibur instrument (BD Biosciences, San Diego, CA) equipped with CellQuest 3.3 Software.

Preparation of cell lysate and western blotting

For the Western blotting, cells (DLD1) were seeded in 6 well plates and treated with different concentrations (4.5 and 9 μM) of compound **23**. After 48 hr of treatment, cells were harvested and washed twice with chilled PBS. The cells were suspended in chilled PBS containing 1x protease inhibitor cocktail and lysed by very brief sonication (2 seconds "On" followed by 10 second "Off" cycle for 3 times) on ice. Sonicated samples were centrifuged at 10,000 rpm for 30 min at 4 °C and lysates were collected and used for Western blot. Protein samples were separated by SDS PAGE and proteins were transferred to PVDF membrane. The membranes were probed with one of the primary antibodies (PCNA, β -actin, γ -H₂AX) while β -actin was used as loading control. Primary antibodies were incubated with appropriate HRP-conjugated secondary antibodies, and developed by enhanced chemiluminescence in Image Quant LAS 4010 (GE Healthcare, Little Chalfont, Buckinghamshire).

Acknowledgements

We acknowledge CSIR (DM, DS, DKS), ICMR (SG, VMB) for research fellowships. This study was financially supported by the ICMR (Indian Council of Medical Research), New Delhi, CSIR-Network project, CSIR (Council of Scientific and Industrial Research), New Delhi, India, Department of Biotechnology (DBT), Govt. of India (Grant-BT/PR6421/GBD/27/436/2012)

ARTICLE

Journal Name

and the Department of Science and Technology (DST), Govt. of India (Grant-SB/FT/LS-163/2012). We acknowledge Mrs. Tara Rawat (STO) for technical assistance and SAIF Division for spectral data. The authors are also thankful to Mr. A.L. Vishwakarma for his support during flow cytometry experiments.

Notes

[§]Both authors contributed equally to this work.

* Corresponding authors: 1. Dr. Vishnu Lal Sharma, Medicinal & Process Chemistry Division, CSIR-Central Drug Research Institute, Sector 10, Jankipuram Extn., Sitapur Road, Lucknow, Uttar Pradesh 226031, India. Tel.: 91-522-2772450; Ext. 4671; Fax: 91-522-2771941 E-mail address: vl_sharma@cdri.res.in; vlscdri@gmail.com.

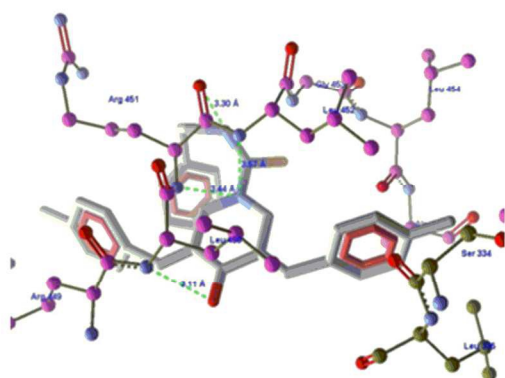
2. Dr. Dibyendu Banerjee, Molecular & Structural Biology Division, CSIR-Central Drug Research Institute, Sector 10, Jankipuram Extn., Sitapur Road, Lucknow, Uttar Pradesh 226031, India, Tel.: 91-522-2772450; Ext. 4443; Fax: 91-522-2771941; E-mail address: d.banerjee@cdri.res.in; dibyendu25@hotmail.com.

References

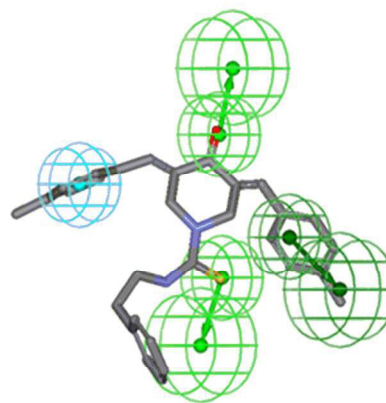
1. J. P. Overington, B. Al-Lazikani and A. L. Hopkins, *Nat. Rev. Drug Discov.*, 2006, **5**, 993-996.
2. C. Holohan, S. Van Schaeybroeck, D. B. Longley and P. G. Johnston, *Nat. Rev. Cancer*, 2013, **13**, 714-726.
3. (a) S. Zhong, X. Chen, X. Zhu, B. Dziegielewska, K. E. Bachman, T. Ellenberger, J. D. Ballin, G. M. Wilson, A. E. Tomkinson and A. D. Mackerell, Jr., *J. Med. Chem.*, 2008, **51**, 4553-4562; (b) X. Chen, S. Zhong, X. Zhu, B. Dziegielewska, T. Ellenberger, G. M. Wilson, A. D. Mackerell, Jr. and A. E. Tomkinson, *Cancer Res.*, 2008, **68**, 3169-3177; (c) M. Srivastava, M. Nambiar, S. Sharma, S. S. Karki, G. Goldsmith, M. Hegde, S. Kumar, M. Pandey, R. K. Singh, P. Ray, R. Natarajan, M. Kelkar, A. De, B. Choudhary and S. C. Raghavan, *Cell*, 2012, **151**, 1474-1487; (d) D. K. Singh, S. Krishna, S. Chandra, M. Shameem, A. L. Deshmukh and D. Banerjee, *Med. Res. Rev.*, 2014, **34**, 567-595; (e) S. Krishna, D. K. Singh, S. Meena, D. Datta, M. I. Siddiqi and D. Banerjee, *J. Chem. Inf. Model.*, 2014, **54**, 781-792; (f) M. Shameem, R. Kumar, S. Krishna, C. Kumar, M. I. Siddiqi, B. Kundu and D. Banerjee, *Chem. Biol. Interact.*, 2015, **237**, 115-124.
4. (a) T. Lindahl and D. E. Barnes, *Annu. Rev. Biochem.*, 1992, **61**, 251-281; (b) A. J. Doherty and S. W. Suh, *Nucleic Acids Res.*, 2000, **28**, 4051-4058; (c) A. Wilkinson, J. Day and R. Bowater, *Mol. Microbiol.*, 2001, **40**, 1241-1248; (d) J. M. Pascal, *Curr. Opin. Struct. Biol.*, 2008, **18**, 96-105; (e) A. E. Tomkinson, S. Vijayakumar, J. M. Pascal and T. Ellenberger, *Chem. Rev.*, 2006, **106**, 687-699.
5. (a) D. E. Barnes, L. H. Johnston, K. Kodama, A. E. Tomkinson, D. D. Lasko and T. Lindahl, *Proc. Natl. Acad. Sci. U. S. A.*, 1990, **87**, 6679-6683; (b) Y. F. Wei, P. Robins, K. Carter, K. Caldecott, D. J. Pappin, G. L. Yu, R. P. Wang, B. K. Shell, R. A. Nash, P. Schar, D. E. Barnes, W. A. Haseltine, and T. Lindahl, *Mol. Cell. Biol.*, 1995, **15**, 3206-3216; (c) A. E. Tomkinson and D. S. Levin, *Bioessays*, 1997, **19**, 893-901. (d) T. Ellenberger and A. E. Tomkinson, *Annu. Rev. Biochem.*, 2008, **77**, 313-338.
6. (a) S. Soderhall, *Eur. J. Biochem.*, 1975, **51**, 129-136; (b) S. Soderhall and T. Lindahl, *J. Biol. Chem.*, 1973, **248**, 672-675.
7. (a) D. S. Levin, W. Bai, N. Yao, M. O'Donnell and A. E. Tomkinson, *Proc. Natl. Acad. Sci. U. S. A.*, 1997, **94**, 12863-12868; (b) R. Prasad, R. K. Singhal, D. K. Srivastava, J. T. Molina, A. E. Tomkinson and S. H. Wilson, *J. Biol. Chem.*, 1996, **271**, 16000-16007; (c) G. L. Dianov, *Am. J. Cancer Res.*, 2011, **1**, 845-851.
8. (a) L. Liang, L. Deng, S. C. Nguyen, X. Zhao, C. D. Maulion, C. Shao and J. A. Tischfield, *Nucleic Acids Res.*, 2008, **36**, 3297-3310; (b) J. Moser, H. Kool, I. Giakzidis, K. Caldecott, L. H. Mullenders and M. I. Foustier, *Mol. Cell*, 2007, **27**, 311-323; (c) T. E. Wilson, U. Grawunder and M. R. Lieber, *Nature* 1997, **388**, 495-498; (d) M. Akbari, G. Keijzers, S. Maynard, M. Scheibye-Knudsen, C. Desler, I. D. Hickson and V. A. Bohr, *DNA Repair (Amst)*, 2014, **16**, 44-53; (e) S. E. Critchlow, R. P. Bowater and S. P. Jackson, *Curr. Biol.*, 1997, **7**, 588-598; (f) U. Grawunder, D. Zimmer, S. Fugmann, K. Schwarz and M. R. Lieber, *Mol. Cell.*, 1998, **2**, 477-484.
9. (a) D. E. Barnes, A. E. Tomkinson, A. R. Lehmann, A. D. Webster and T. Lindahl, *Cell*, 1992, **69**, 495-503; (b) A. D. Webster, D. E. Barnes, C. F. Arlett, A. R. Lehmann and T. Lindahl, *Lancet*, 1992, **339**, 1508-1509; (c) C. Prigent, M. S. Satoh, G. Daly, D. E. Barnes and T. Lindahl, *Mol. Cell. Biol.*, 1994, **14**, 310-317; (d) C. L. Hsieh, C. F. Arlett and M. R. Lieber, *J. Biol. Chem.*, 1993, **268**, 20105-20109.
10. J. M. Pascal, P. J. O'Brien, A. E. Tomkinson and T. Ellenberger, *Nature* 2004, **432**, 473-478.
11. (a) A. Montecucco, G. Biamonti, E. Savini, F. Focher, S. Spadari and G. Ciarrocchi, *Nucleic Acids Res.*, 1992, **20**, 6209-6214; (b) D. Sun, R. Urrabaz, M. Nguyen, J. Marty, S. Stringer, E. Cruz, L. Medina-Gundrum and S. Weitman, *Clin. Cancer Res.*, 2001, **7**, 4143-4148.
12. S. Satbhaiya and O. P. Chourasia, *RSC Adv.*, 2015, **5**, 84810-84820.
13. <http://www.fda.gov/ScienceResearch/SpecialTopics/CriticalPathInitiative/CriticalPathOpportunitiesReports/ucm077262.htm> (accessed on 10.10.2015)
14. (a) T. T. Feng, W. L. Chen, D. D. Li, H. Z. Lin, F. Liu, Q. C. Bao, Y. H. Lei, X. J. Zhang, X. L. Xu, X. K. Guo, Q. D. You and H. P. Sun, *RSC Adv.*, 2015, **5**, 82936-82946; (b) G. Khodarahmi, P. Asadi, H. Farrokhpour, F. Hassanzadeh and M. Dinari, *RSC Adv.*, 2015, **5**, 58055-58064; (c) V. P. Zambre, V. A. Hambarde, N. N. Petkar, C. N. Patel and S. D. Sawant, *RSC Adv.*, 2015, **5**, 23922-23940; (d) N. Jain, S. Gupta, N. Sapre and N. S. Sapre, *RSC Adv.*, 2015, **5**, 14814-14827; (e) R. J. Li, X. L. Su, Z. Chen, W. X. Huang, Y. L. Wang, K. B. Wang, B. Lin, J. Wang and M. S. Cheng, *RSC Adv.*, 2015, **5**, 23202-23209; (f) H. M. Patel, P. Bari, R. Karpoomath, M. Noolvi, N. Thapliyal, S. Surana and P. Jain, *RSC Adv.*, 2015, **5**, 56724-56771.
15. S. Singh, B. K. Malik and D. K. Sharma, *Bioinformation*, 2006, **1**, 314-320.

16. X. Wang, Y. Zhang, X. Zhang, W. Tian, W. Feng and T. Chen, *Int. J. Oncol.*, 2012, **40**, 1189-1195.
17. (a) K. Bairwa, J. Grover, M. Kania and S. M. Jachak, *RSC Adv.*, 2014, **4**, 13946-13978; (b) C. D. Mock, B. C. Jordan and C. Selvam, *RSC Adv.*, 2015, **5**, 75575-75588; (c) A. Anthwal, K. Singh, M. S. M. Rawat, A. K. Tyagi, B. B. Aggarwal and D. S. Rawat, *RSC Adv.*, 2014, **4**, 28756-28764.
18. L. P. Wen, J. A. Fahrni, S. Troie, J. L. Guan, K. Orth and G. D. Rosen, *J. Biol. Chem.*, 1997, **272**, 26056-26061.
19. L. J. Kuo and L. X. Yang, *In Vivo*, 2008, **22**, 305-309.
20. F. J. Kubben, A. Peeters-Haesevoets, L. G. Engels, C. G. Baeten, B. Schutte, J. W. Arends, R. W. Stockbrugger and G. H. Blijham, *Gut*, 1994, **35**, 530-535.
21. P. Lagisetty, P. Vilekar, K. Sahoo, S. Anant and V. Awasthi, *Bioorg. Med. Chem.*, 2010, **18**, 6109-6120.
22. R. Thomsen and M. H. Christensen, *J. Med. Chem.*, 2006, **49**, 3315-3321.
23. D. K. Gehlhaar, G. M. Verkhivker, P. A. Rejto, C. J. Sherman, D. B. Fogel, L. J. Fogel and S. T. Freer, *Chem. Biol.*, 1995, **2**, 317-324.
24. Gehlhaar, D. K.; Bouzida, D.; Rejto, P.A.; 1998. Fully automated and rapidflexible docking of inhibitors covalently bound to serine proteases in evolutionary programming VII. In: Proceedings of the Seventh International Conference on Evolutionary Programming. London, UK: Springer, pp. 449-461.
25. Catalyst, release version 4.1; Accelrys Inc.: San Diego, CA, 2006.
26. A. Saxena, V. M. Balaramnavar, T. Hohlfeld and A. K. Saxena, *Eur. J. Pharmacol.*, 2013, **721**, 215-224.
27. A. K. Saxena, J. Devillers, A. R. Pery, R. Beaudouin, V. M. Balaramnavar and S. Ahmed, *SAR QSAR Environ. Res.*, 2014, **25**, 407-421.
28. K. K. Ramakrishna, S. Gunjan, A. K. Shukla, V. R. Pasam, V. M. Balaramnavar, A. Sharma, S. Jaiswal, J. Lal, R. Tripathi, Anubhooti, R. Ramachandran and R. P. Tripathi, *ACS Med. Chem. Lett.*, 2014, **5**, 878-883.
29. V. M. Balaramnavar, R. Srivastava, N. Rahuja, S. Gupta, A. K. Rawat, S. Varshney, H. Chandasana, Y. S. Chhonker, P. K. Doharey, S. Kumar, S. Gautam, S. P. Srivastava, R. S. Bhatta, J. K. Saxena, A. N. Gaikwad, A. K. Srivastava and A. K. Saxena, *Eur. J. Med. Chem.*, 2014, **87**, 578-594.
30. C. S. Azad, V. M. Balaramnavar, I. A. Khan, P. K. Doharey, J. K. Saxena and A. K. Saxena, *RSC Adv.*, 2015, **5**, 82208-82214.
31. K. V. Sashidhara, S. R. Avula, P. K. Doharey, L. R. Singh, V. M. Balaramnavar, J. Gupta, S. Misra-Bhattacharya, S. Rathaur, A. K. Saxena and J. K. Saxena, *Eur. J. Med. Chem.*, 2015, **103**, 418-428.
32. X. Chen, J. Pascal, S. Vijayakumar, G. M. Wilson, T. Ellenberger and A. E. Tomkinson, *Methods Enzymol.*, 2006, **409**, 39-52.
33. A. S. Cardew and K. R. Fox, *Methods Mol. Biol.*, 2010, **613**, 153-172.

Table of Contents:



Binding modes of compound 23 with hLigI



Compound 23 in designed pharmacophore model

This study reported the generation of a pharmacophore model for the discovery of a novel class of human DNA ligase I inhibitors to target cancer. Thirty six compounds were synthesized and the identified inhibitor, compound **23** Shown anti-ligase activity at low IC_{50} value 24.9 μM as compared to standard curcumin (51.9 μM). It was exhibited good anti-cancer activity and inhibited the ligation activity by abolishing the interaction between hLigI and DNA.